Journal Pre-proofs

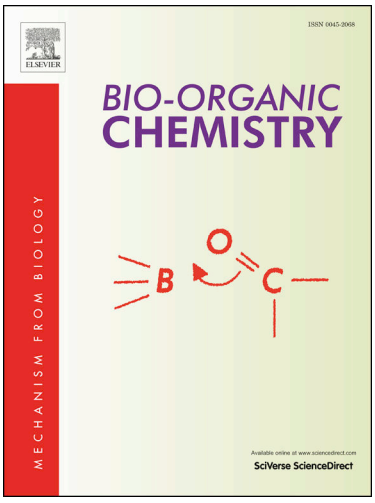

Arylidenes of Quinolin-2-one scaffold as Erlotinib analogues with activities against leukemia through inhibition of EGFR TK/ STAT-3 pathways

Mohammed A.I. Elbastawesy, Mohamed Ramadan, Yaseen A.M.M. El-Shaier, Ashraf A. Aly, Gamal El-Din A. Abuo-Rahma

PII: S0045-2068(19)31912-1
DOI: https://doi.org/10.1016/j.bioorg.2020.103628
Reference: YBIOO 103628

To appear in: *Bioorganic Chemistry*

Received Date: 9 November 2019
Revised Date: 21 December 2019
Accepted Date: 25 January 2020

Please cite this article as: M.A.I. Elbastawesy, M. Ramadan, Y.A.M. El-Shaier, A.A. Aly, G.E-D. Abuo-Rahma, Arylidenes of Quinolin-2-one scaffold as Erlotinib analogues with activities against leukemia through inhibition of EGFR TK/ STAT-3 pathways, *Bioorganic Chemistry* (2020), doi: https://doi.org/10.1016/j.bioorg.2020.103628

Arylidenes of Quinolin-2-one scaffold as Erlotinib analogues with activities against leukemia through inhibition of EGFR TK/ STAT-3 pathways

Mohammed A. I. Elbastawesy,[a] Mohamed Ramadan,[a] Yaseen A. M. M. El-Shaier,[b] Ashraf A. Aly,[c]* Gamal El-Din A Abuo-Rahma[d]*

[a]Department of Pharmaceutical Organic Chemistry, Faculty of Pharmacy, Al-Azhar University, 71524 Assiut, Egypt [b]Department of Organic and Medicinal Chemistry, Faculty of Pharmacy, University of Sadat City, Sadat-City, Menufia, Egypt, [c] Department of Chemistry, Faculty of Science, Minia University, 61519 Minia, Egypt,.[d]* Department of Medicinal Chemistry, Faculty of Pharmacy, Minia University, 61519 Minia, Egypt*

: **To whom correspondence should be addressed:*

*A. A. Aly: ashrafaly63@yahoo.com, +201006268742

* G. E-D. A. Abuo-Rahma: gamal.aborahama@mu.edu.eg, +201003069431

Abstract

A new series of 6-substiuted-4-(2-(4-substituted-benzylidene)hydrazinyl)quinolin-2(1*H*)-one derivatives have been designed and synthesized. The structure of the synthesized compounds was proved by ^{1}H NMR, ^{13}C NMR, 2D NMR, mass and elemental analyses. The target compounds were evaluated for their *in vitro* cytotoxic activity against 60 cancer cell lines according to NCI protocol. Consequently, the most active compounds were further examined against the most sensitive leukemia RPMI-8226 and on healthy cell lines. 6-Chloro-derivative was the most active one; with IC_{50} = 15.72±1.21 and 46.05±2.36 μM against RPMI-8226 and normal cell lines, respectively. Also, it showed a remarkable inhibitory activity compared to gefitinib on the EGFR TK mutant, wild and on H-RAS in addition to STAT-3 with IC_{50} = 695.49±21.8, 263.15±15.13, 10.61±0.27 and 1.753±0.81 nM, respectively. Cell cycle analysis of RPMI-8226 cells treated with the 6-chloro-derivative showed cell cycle arrest at G2/M phase (supported by Caspases-3,8, BAX and Bcl-2 studies) with a significant pro-apoptotic activity as indicated by annexin V-FITC staining. Moreover, the docking studies (modeling, ROCS and Tanimoto scores) supported the results; the study illustrated the effect of several factors on compounds activity.

Keywords: Quinolin-2-one, Antiproliferative; Molecular docking, EGFR- TK; STAT, RAS, apoptotic, Docking; Openeye.

1. Introduction

Quinolones represents an interesting class as one of the nitrogen containing heterocycles. They also constitute indispensable structural units in medicinal chemistry. Among various heterocyclic compounds, researchers all over the world have been interested in the biological applications of quinolone derivatives [1,2]. In recent years, the quinolone bioisoster, quinazoline derivatives like gefitinib and erlotinib (**Figure 1**) have been approved by the FDA as EGFR kinase inhibitors for the treatment of non-small cell lung and breast cancer [3-5]. Modification of scaffold with different substituents is a general method for the drug design and development [6,7] with the possibility of obtaining more successful next generation derivatives [8]. Recently many groups [9-11] reported that bioisosteric replacement of the quinazoline core with quinoline-2-one ring, afforded many new compounds (e.g. **PQ-1** and **PQ-2**, **Figure 1**) with potent EGFR kinase inhibitory activity and remarkable apoptotic activities [11,12].

Schiff base moiety which is characterized by the presence of azomethine group (-C=N-) is an exceptionally adaptable drug-like format that is being utilized broadly in the structure of cancer treatments and cellular apoptosis [13-16]. These compounds exhibit anticancer activity by the restraint of various kinds of enzymes [17], proteins [18] and receptors [19] which assume basic roles in cell division [20].

Research and development of new anticancer therapeutic agents are of paramount importance because of the innate ability of tumor cells to develop resistance to existing therapies [21]. The progression of multiple drug resistance to anticancer agents in human tumor cells has been recognized as major impediment to unbeaten cancer chemotherapy [22]. Thus, studies for the identification of novel drugs and targets for the management of such diseases are at the cutting edge. The hybridization of biologically active molecules is a powerful tool for the drug discovery used to target a variety of diseases [23, 24]. In continuation to our previous works on

the quinolone scaffold [11,25-27], the target compounds were elaborated utilizing molecular modeling approaches [11]. The design strategy of the present study (**Figure 1**) is constructed based on the well-known biologically active entities quinoline-2-one with Schiff base hopping synergistic improvement of the designed molecules as antitumor agents. To investigate the possible anticancer mechanism of the synthesized compounds; EGFR, STAT and RAS enzymatic assay was performed. Molecular docking study of the most active compounds inside the active site of EGFR enzyme was done. Cell cycle analysis and apoptosis through caspase-3, and 8 expression levels were screened, in addition to expression level of Bax and Bcl-2.

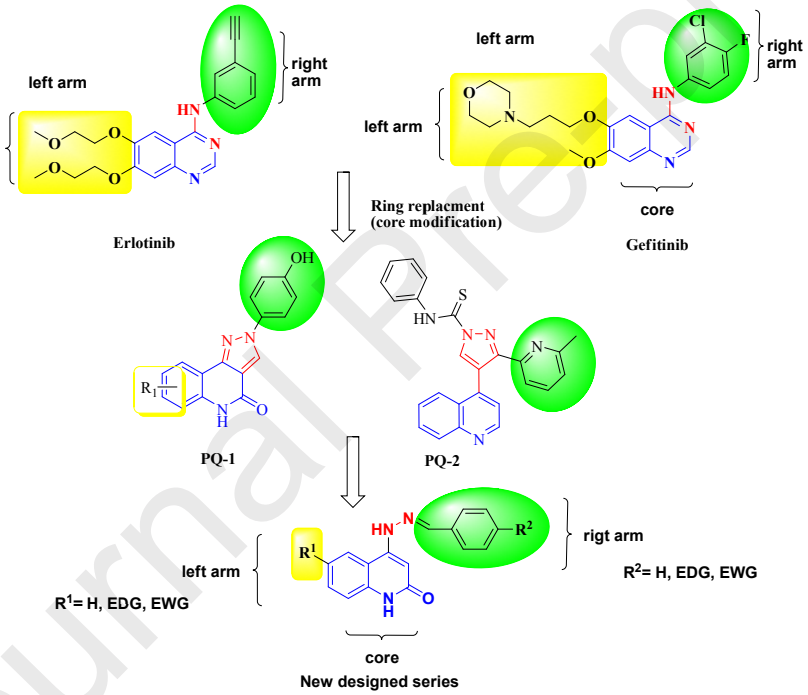

Figure 1. Rational for the design of the target compounds.

2. Results and discussion

2.1. Chemistry

The target compounds **6a-o** were prepared according to **Scheme 1**. Compounds **1-5** were synthesized according to the reported method [28-30] and their structures were confirmed by matching their spectral data with the reported ones [30] . The key intermediates 4-hydrazino-

quinolin-2-ones **5a-c** were prepared by heating at reflux compounds **4a-c** with hydrazine hydrate for nearly 10-15 h [31]. Refluxing **5a-c** with different aldehyde derivatives in presence of acetic acid as catalyst furnished the target 6-substiuted-4-(2-(4-substituted-benzylidene)hydrazinyl)-quinolin-2(1*H*)-ones **6a-o** (Scheme 1).

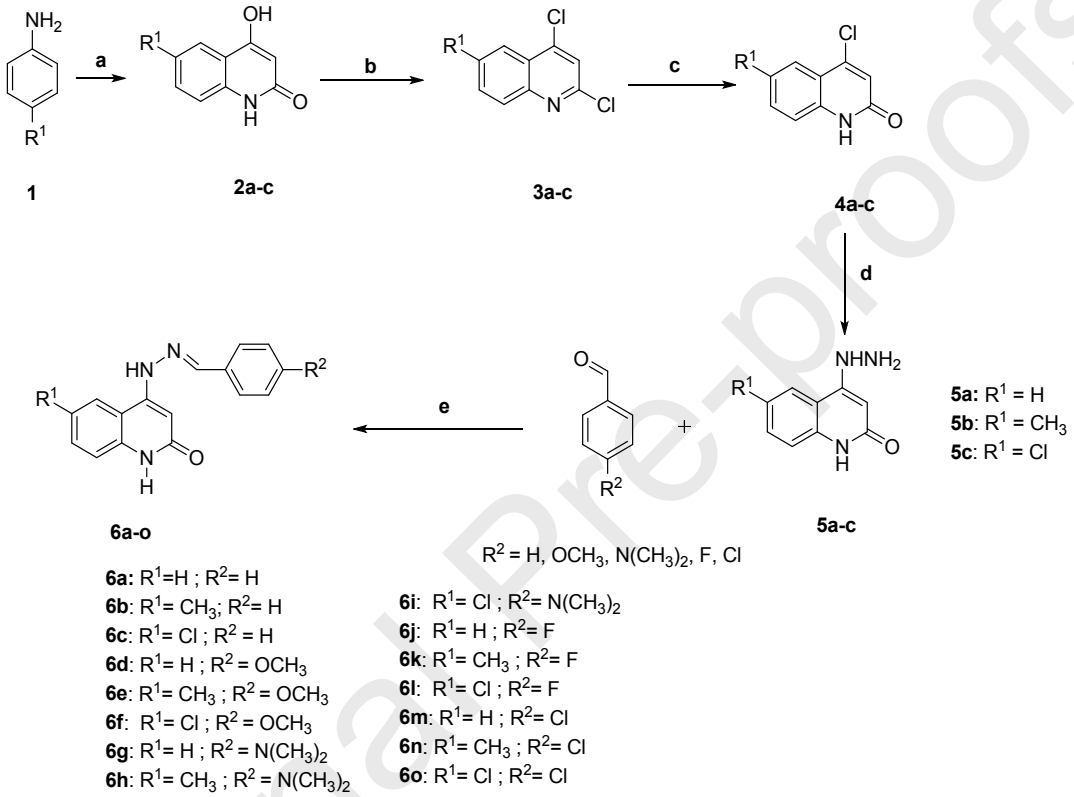

Scheme 1. Synthesis of target compounds **6a-o**

Reagent and reaction conditions: a) Diethyl malonate, PPA, reflux 3 h; b) $POCl_3$, reflux 2 h; c) AcOH, reflux 10 h; d) $NH_2NH_2 \cdot H_2O$ (85%), EtOH, reflux 10-15 h; e) AcOH, EtOH, reflux 5-8 h.

The spectral and elemental data results revealed that all **6a-o** derivatives underwent the reaction smoothly to give the respective Schiff base-quinoline-2-one structure in 70-95% yield.^{1}H NMR spectra experienced the disappearance of NH_2 signal and appearance of doublet of doublet characteristic pattern in aromatic δ 6.70-8.00 ppm region which augments formation of Schiff

base. As a representative example, compound **6h**, NMR spectra showed a singlet signals at δ10.89 and 10.42 ppm for two NH groups. Also as mentioned; a characteristic pattern for the additional four phenyl protons at δ 7.56 and 6.77 ppm represented di para substituted phenyl. Moreover, 6H singlet signal at δ 2.98 which distinctive as dimethylamino protons. The distinguished azomethine CH proton appeared at δ 8.26 ppm their attached carbons which resonate at δ_C 39.78 ppm gives HMBC correlation with the nitrogen at δ_N 52.8, also with a non-protonated carbon at δ_C 151.14, assigned as para phenyl carbon. Moreover, the imine carbon appears at δ_C 144.60. represents (C=N) moiety giving HMBC correlation with the sp^2 nitrogen at δ_N 308.2, assigned as N-4c, and with one of the two co-resonant nitrogens at δ_N 140.4, assigned as N-4b (**Table 1**).

Table 1: NMR spectroscopic assignments of compound **6h**

^{1}H NMR		**COSY**	**Assignment**
10.89 (s; 1H)		*6.14*	H-1
10.42 (s; 1H)			H-4b
8.26 (s; 1H)			H-4d
7.85 (s; 1H)		*7.31, 2.38*	H-5
7.56 (d, *J* = 8.8; 2H)		6.77	H-*o*
7.31 (d, *J* = 8.4; 1H)		*7.85,* 7.18, *2.38*	H-7
7.18 (d, *J* = 8.3; 1H)		7.31	H-8
6.77 (d, *J* = 8.8; 2H)		7.56	H-*m*
6.14 (s; 1H)		*10.89*	H-3
2.98 (s; 6H)			H-*p"*
2.38 (s; 3H)		*7.85, 7.31*	H-6a
^{15}N NMR	**HSQC**	**HMBC**	**Assignment**
308.2		10.42, 8.26	N-4c
140.4	10.89	7.18, 6.14	N-1
140.4	10.42	8.26, 6.14	N-4b
52.8		6.77, 2.98	N-*p'*

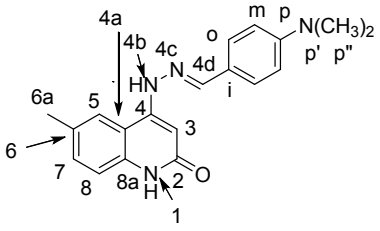

^{13}C NMR	**HSQC**	**HMBC**	**Assignment**
162.80		*10.42*	C-2
151.14		7.56, 2.98	C-*p*
148.18		10.42, 7.85, 7.18, 6.14	C-4
144.60	8.26	10.42, 7.56	C-4d
137.34		7.85, 7.31, *7.18, 2.38*	C-8a
131.31	7.31	7.85, 2.38	C-7
129.45		7.85, 7.18, *2.38*	C-6
127.85	7.56	7.56	C-*o*
122.20		8.26, 6.77	C-*i*
121.38	7.85	7.31, *7.18,* 2.38	C-5

115.53	7.18		C-8
111.94	6.77	7.56, 6.77, 2.98	C-*m*
111.79		10.89, 10.42, 7.18, 6.14	C-4a
93.17	6.14	10.89, 10.42	C-3
39.78	2.98	2.98	C-*p"*
20.64	2.38	7.85, 7.31	C-6a

The mass spectra and elemental analyses indicated that the molecular weight is consistent with the molecular formula of the target compounds. In another example, ^{1}H NMR spectrum of **6j** showed a broad singlet signals at δ 11.17 and 10.83 ppm (disappeared upon deterioration) represent both NH protons. A doublet of doublet pattern at δ 7.80, 7.30 ppm ascribed for four phenyl protons.^{13}C NMR spectrum of **6j** showed peak at δ 162.25 ppm assigned for the C-F carbon. In addition, other signals at δ142.08 ppm for (C=N) group and peak at δ 160.70 ppm assigned to the (C=O) of the quinoline-2-one moiety.

2.2. Biology

2.2.1 Evaluation of *in vitro* antiproliferative activity for compounds 6a-o.

The target compounds **6a-o** were selected by National Cancer Institute (NCI, Bethesda, ML, USA (http://www.dtp.nci.nih.gov.) for evaluation at single concentration of 10 μM towards panel of sixty cancer cell lines of nine diverse tissues according to NCI protocol, **Appendix A**. The screening results were reported as the percent growth inhibition of treated cells compared to untreated control cells. Results in **Table 2** revealed that most compounds showed weak to moderate activities on most tested cell lines specially leukemia and small cell lung cancer cell lines. Compounds **6c** showed promising activity on **EKVX** cell line achieving 53.96% of growth inhibition. On other hand, compound **6f** showed the widest activity on such cell line achieving 59.77, 79.48, 76.11 and -42.75 % on **A549/ATCC, NCI-H23, NCI-H460** and **NCI-H522** respectively. Compound **6l** was the most active on non-small lung cancer cell line achieving -48.31% against **HOP-92** cell line. Moreover, the results on leukemia cell line was

remarkable; specially with compounds **6f** and **6l** which were the most active, achieving high activity on all the tested cell lines.

It is obvious that the electronic effect on both position of substituent on the tested scaffolds had a pronounced effect on their cytotoxic activity. Compound **6f** with electron withdrawing group on quinoline-2-one scaffold has showed higher antiproliferative activity on all tested cell lines than compound **6d** and **6e** with electron donating groups (**Table 2**). Also, compound **6l** with chlorine substituted on quinoline-2-one 6 position showed approximately a complete inhibition on all leukemia cell lines exceeding **6j** and **6k** with H or methyl substitution on the same quinoline-2-one ring position. Substitutions on phenyl ring of Schiff bases also altering the activity of such derivatives. Compounds **6j-l** with florin group showed the highest activity against leukemia cell line among the entire tested group. Also compounds **6j-o** with the electron withdrawing phenyl groups showed higher activities than **6d-6i** with electron donating groups and then **6a-c** with no substitution at all. From the results, it is clear that substitution on the quinoline-2-one is important for the antiproliferative activity especially with electron withdrawing groups. Moreover, substitution on the phenyl terminal part increases the activity also with electron withdrawing group like fluorine. The maximum biological effect has gained in compound **6l** with chlorine and fluorine atom in both positions, achieving the highest results among all tested compounds with complete inhibition of the tested leukemia cancer cell lines (**Table 2).**

Table 2. Percentage growth inhibition (GI %) of *in vitro* subpanel tumor cell lines at 10 μM concentration for compounds **6a-o**.

Subpanel cancer cell Lines	% Growth Inhibition (GI %)[a]														
	6a	**6b**	**6c**	**6d**	**6e**	**6f**	**6g**	**6h**	**6i**	**6j**	**6k**	**6l**	**6m**	**6n**	**6o**
Leukemia															
CCRF-CEM	12.91	12.60	-	-	12.00	**61.76**	-	12.42	-	16.74	32.94	113.24	-	-	30.88
HL-60(TB)	22.34	21.04	13.81	-	-	**54.73**	-	-	-	35.07	24.43	109.23	10.73	-	-
K-562	23.02	29.20	25.20	-	20.54	**79.05**	-	17.12	-	47.64	34.73	**97.62**	28.87	-	33.23
MOLT-4	20.87	22.81	10.41	-	20.98	**69.71**	-	24.02	12.90	27.88	42.18	115.79	12.34	-	22.98
RPMI-8226	21.69	19.99	22.44	-	18.39	**63.41**	-	15.43	-	27.04	31.25	143.18	-	-	21.30
-small cell lung cancer															
A549/ATCC	14.73	14.82	10.83	-	-	**59.77**	-	-	-	-	11.62	10.67	-	-	14.43
EKVX	10.86	24.67	**53.96**	-	18.03	36.19	-	14.45	14.29	13.01	42.63	25.83	-	11.06	29.11
HOP-62	-	10.78	-	11.17	13.74	28.10	-	11.34	-	-	14.33	-	-	-	-
HOP-92	24.22	30.13	-	11.97	12.05	29.23	21.02	23.23	17.81	22.99	-	148.31	-	18.37	-
NCI-H226	-	16.25	-	-	18.55	19.62	24.01	17.09	25.03	-	22.65	23.87	-	-	18.72
NCI-H23	13.93	24.27	13.87	16.07	29.96	**79.48**	-	15.66	17.21	21.29	-	14.75	-	-	22.26
NCI-H322M	-	-	-	-	13.24	33.71	-	-	-	-	11.02	-	-	-	-
NCI-H460	-	13.22	-	-	-	**76.11**	-	-	-	14.56	15.59	-	-	-	18.18
NCI-H522	18.00	16.13	19.65	24.50	24.76	**142.75**	12.89	12.89	13.95	21.16	33.78	27.19	20.71	14.88	43.89
n cancer															
COLO 205	-	-	-	-	-	16.72	-	-	-	-	14.49	-	-	-	-
HCC-2998	-	-	13.81	16.84	-	11.16	-	-	-	-	-	14.93	-	18.42	-
HCT-116	-	10.75	15.03	21.13	16.86	**91.08**	13.11	24.28	11.60	18.54	25.08	15.93	-	10.54	-
HCT-15	-	-	-	-	12.11	**60.48**	-	11.28	-	13.34	20.96	16.60	-	-	28.84
HT29	11.13	-	-	-	-	**96.71**	-	-	-	12.18	13.43	11.64	11.26	-	11.87
KM12	-	-	-	-	-	**53.44**	-	-	-	13.51	-	-	-	-	10.24
SW-620	10.10	-	-	-	-	**62.11**	-	-	14.02	11.47	14.05	-	-	-	17.47
cancer															
SF-268	-	-	-	-	-	41.08	-	-	-	-	-	-	-	-	-
SF-295	-	-	-	-	-	27.44	-	-	-	-	10.02	-	-	-	15.90
SF-539	-	-	-	-	-	-	-	-	-	-	-	-	-	-	-
SNB-19	-	-	-	-	-	14.22	-	-	-	-	-	-	-	-	-
SNB-75		-	-	13.36	-	-	23.44	22.29	21.55	-	-	-	-	-	-
U251	-	-	-	-	-	**71.12**	-	-	-	-	-	-	-	-	14.04
noma															
LOX IMVI	-		-	-	-	**62.83**	-	-	-	-	-	-	-	-	-
MALME-3M	-	-	-	-	-	**54.02**	-	-	-	-	-	-	-	-	-

M14	15.44	13.65	11.85	11.93	13.75	45.19	10.98	10.40	-	19.78	20.55	18.85	-	-	10.43
MDA-MB-43	-	-	-	-	-	**56.77**	-	-	-	35.94	27.68	21.37	-	-	33.23
SK-MEL-2	-	14.68	22.20	-	19.33	**51.20**	-	20.67	-	16.67	22.23	22.78	-	-	10.58
SK-MEL-28	-	-	-	-	-	12.81	-	-	-	-	-	10.04	-	-	-
SK-MEL-5	12.07	22.56	31.14	-	31.02	**61.77**	-	12.37	-	12.45	45.26	88.45	10.86	**51.12**	**75.81**
UACC-257	10.43	-	-	-	-	18.26	-	-	-	12.08	15.81	14.22	15.39	-	19.10
UACC-62	12.12	13.25	-	-	10.57	22.69	13.76	10.71	17.87	-	18.18	19.56	-	10.65	20.76
rian cancer															
IGROV1	-	-	-	-	-	24.26	20.45	18.92	24.73	-	-	-	-	-	-
OVCAR-3	-	-	-	-	-	**89.18**	-	-	-	-	-	-	-	-	-
OVCAR-4	-	-	-	-	-	**56.94**	-	-	-	-	-	-	-	-	15.22
OVCAR-5	-	11.13	14.07	-	-	-	-	-	-	-	-	11.56	-	-	-
OVCAR-8	-	10.71	-	-	-	30.88	-	-	-	-	-	-	-	-	10.68
NCI/ADR-RE	-	-	-	16.63	-	21.95	-	-	-	-	-	-	-	-	-
SK-OV-3	13.30	18.16	-	-	12.44	-	15.02	15.91	17.10	10.86	24.82	15.08	22.20	-	-
al cancer															
786-0	-	-	-	-	-	37.86	-	-	-	-	10.42	10.50	-	-	-
A498	11.07	18.87	12.24	-	12.33	19.29	-	-	-	-	25.84	-	-	-	-
ACHN	-	18.25	-	-	-	27.31	-	-	-	-	-	-	-	-	14.96
CAKI-1	15.27	10.21	-	-	-	13.84	-	12.76	-	-	-	-	-	-	15.04
RXF 393	-	-	-	-	-	14.37	-	-	-	-	-	-	-	-	-
SN12C	-	-	-	-	11.68	37.67	-	-	-	-	10.48	-	-	-	-
TK-10	-	-	-	-	-	**87.45**	-	-	-	-	-	-	-	-	-
UO-31	17.40	25.42	12.81	-	24.25	-	34.45	32.27	32.11	-	14.84	20.99	-	-	-
tate cancer															
PC-3	21.04	25.22	21.40	-	20.93	40.92	13.63	19.60	13.65	22.84	24.14	143.04	12.31	12.07	22.91
DU-145	-	-	-	-	-	35.34	-	-	-	-	-	-	-	-	-
ıst cancer															
MCF7	23.74	29.09	13.26	-	21.93	**64.82**	-	23.10	19.04	14.67	-	15.4	-	-	31.81
MDA-MB-231/ATCC	-	-	-	-	-	28.67	-	14.48	-	-	-	-	-	-	25.43
HS 578T	-	13.86	17.45	-	11.68		17.75	15.60	17.23	-	13.92	-	-	-	-
BT-549	13.02	-	-	-	11.68	**67.92**	10.57	13.72	14.53	-	-	-	-	-	-
T-47D	23.75	22.12	24.13	11.29	29.26	**57.56**	21.29	20.27	18.33	19.07	30.83	31.48	-	-	15.68
MDA-MB-46	-	20.24	22.66	-	-	22.04	-	-	-	-	-	27.05	-	18.08	31.17

(–): Weak activity GI < 10%.

2.2.2. *In vitro* five dose full NCI 60 cell panel assay

Compounds **6l** was selected for five dose testing against the full panel of 60 human tumor cell lines according to NCI protocol (http://www.dtp.nci.nih.gov.). All the 60 cell lines representing nine

tumor subpanels were incubated at five different concentrations (0.01, 0.1, 1, 10, and 100 μM). The outcomes were used to form log concentration *vs* % growth inhibition curves and three response parameters (GI_{50}, TGI, and LC_{50}) were calculated for each cell line. The GI_{50} value (growth inhibitory activity) corresponds to the concentration of the compound causing 50% decrease in net cell growth, the TGI value (cytostatic activity) is the concentration of the compound resulting in total growth inhibition (TGI) and LC_{50} value (cytotoxic activity) is the concentration of the compound causing net 50% loss of initial cells at the end of the incubation period of 48 h. The principle for selectivity of compound depends upon the ratio obtained by dividing the full panel MID (the average sensitivity of all cell lines toward the test agent) (μM) by their individual subpanel MID (μM). Ratios between 3 and 6 refer to moderate selectivity; ratios > 6 indicate high selectivity toward the corresponding cell line, whilst compounds not meeting either of these criteria rated nonselective, **Appendix A**.

Compound **6l** exhibited noteworthy antiproliferative activity against all cancer cell lines with low selectivity ratios. Leukemia, melanoma, breast and small cell lung cancers were the most affected tissues. Compound **6l** achieved its highest results against MOLT-4 leukemia cell line with GI_{50} of 4.07 μM (**Table 3**) with selectivity ratio of 1.32 and GI_{50} against SK-MEL-5 melanoma cancer equal to 3.55 and selectivity ratio 1.30.

$$\textbf{Selective index} = \frac{\textbf{MIDa}}{\textbf{MIDb}}.$$

Table 3. Results of *in vitro* five doses testing of nine human cancer types and selectivity for compounds **6l**.

		6l				
		GI_{50}				
Panel	**Cell line**	**Conc. per cell line**	**MID[b]**	**Selectivity ratio**	**TGI**	**LC_{50}**
Leukemia	CCRF-CEM	**12.0**	**14.94**	**1.32**	> 100	> 100
	HL-60(TB)	**18.9**			**50.9**	> 100
	K-562	**13.2**			**93.2**	> 100
	MOLT-4	**4.07**			> 100	> 100
	RPMI-8226	**17.0**			> 100	> 100
Non-small cell lung cancer	SR	**24.5**	**18.79**	**1.05**	**85.6**	> 100
	A549/ATCC	**23.5**			> 100	> 100
	EKVX	**16.8**			> 100	> 100
	HOP-62	**20.8**			> 100	> 100
	HOP-92	**14.0**			**45.9**	> 100
	NCI-H226	**14.6**			> 100	> 100
	NCI-H23	**19.5**			**76.1**	> 100
	NCI-H322M	**22.2**			> 100	> 100
	NCI-H460	**20.3**			> 100	> 100
	NCI-H522	**17.4**			**74.3**	> 100
Colon Cancer	COLO 205	**18.2**	**22.83**	**0.86**	**43.5**	> 100
	HCC-2998	**32.4**			> 100	> 100
	HCT-116	**17.4**			> 100	> 100
	HCT-15	**19.9**			> 100	> 100
	HT29	**23.1**			> 100	> 100
	KM12	**22.0**			> 100	> 100
	SW-620	**26.8**			> 100	> 100
CNS Cancer	SF-268	**33.6**	**22.75**	**0.87**	> 100	> 100
	SF-295	**21.9**			> 100	> 100
	SF-539	**23.6**			**78.2**	> 100
	SNB-19	**23.5**			> 100	> 100
	SNB-75	**12.8**			**83.1**	> 100
	U251	**21.1**			**98.4**	> 100
Melanoma	LOX IMVI	**25.3**	**15.23**	**1.30**	> 100	> 100
	MALME-3M	**14.2**			**54.0**	> 100
	M14	**10.2**			> 100	> 100

Ovarian Cancer	MDA-MB-435	**13.5**	**21.38**	**0.92**	> 100	> 100
	SK-MEL-2	**18.3**			**69.3**	> 100
	SK-MEL-28	**19.8**			> 100	> 100
	SK-MEL-5	**3.55**			**14.1**	> 100
	UACC-257	**15.5**			**56.5**	> 100
	UACC-62	**16.7**			> 100	> 100
	IGROV1	**18.5**			> 100	> 100
	OVCAR-3	**24.8**			> 100	> 100
	OVCAR-5	**21.6**			**58.9**	> 100
	OVCAR-8	**19.8**			> 100	> 100
	NCI/ADR-RES	**23.5**			> 100	> 100
	SK-OV-3	**20.1**			**83.4**	> 100
Renal Cancer	786-0	**26.3**	**24.78**	**0.80**	> 100	> 100
	A498	**14.8**			**92.7**	> 100
	ACHN	**17.2**			**72.1**	> 100
	CAKI-1	**23.5**			> 100	> 100
	RXF 393	**23.7**			> 100	> 100
	SN12C	**23.8**			> 100	> 100
	TK-10	**47.1**			> 100	> 100
	UO-31	**21.9**			> 100	> 100
Prostate Cancer	PC-3	**8.41**	**21.15**	**0.93**	**96.3**	> 100
	DU-145	**33.9**			> 100	> 100
Breast Cancer	MCF7	**15.3**	**17.38**	**1.14**	> 100	> 100
	MDA-MB-231/ATCC	**16.0**			**51.7**	> 100
	HS 578T	**25.3**			> 100	> 100
	BT-549	**15.8**			**44.5**	> 100
	T-47D	**18.6**			> 100	> 100
	MDA-MB-468	**13.3**			**49.1**	> 100

MID[a] for **6l** = 19.75

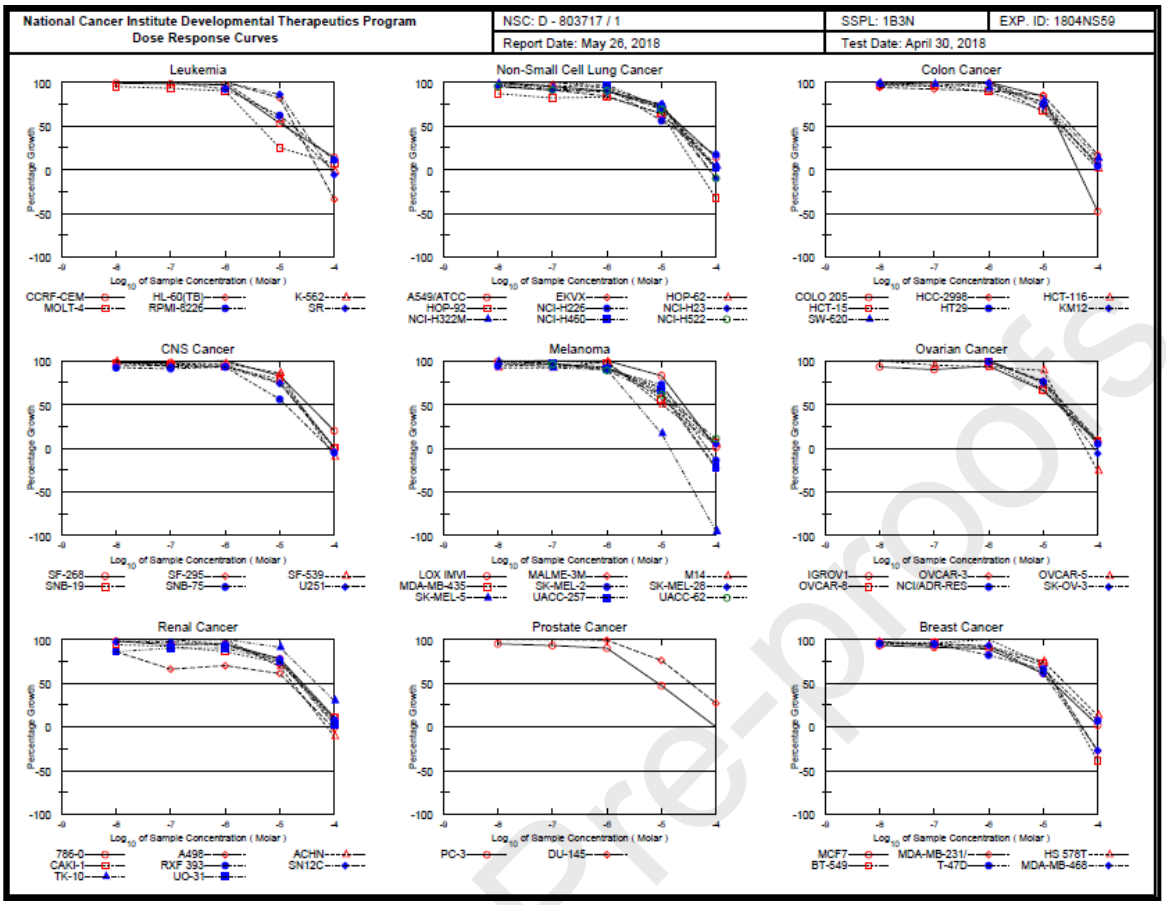

Figure 2. Dose-antiproliferative response of compound **6l** against nine different cancer cell lines

2.2.3. Cytotoxic activity evaluation of IC_{50}

Independently, compound **6l** was selected for further investigation, it was evaluated for its anticancer activity against RPMI-8226 leukemia cancer and on normal healthy unaffected cell lines by MTT assay (**Appendix A**) [32] (**Table 4**). Compound **6l** achieved **IC_{50}**=15.72±1.21 **µM** on the selected RPMI-8226 leukemia cancer cell lines which is considered a comparable result with the reference gefitinib **IC_{50}**= 9.92±0.62 **µM**.

Same approach happened in normal healthy cells; **6l** showed **IC_{50}**= 46.05±2.36 **µM** and gefitinib achived **IC_{50}**= 33.49±1.73 **uM,** which indicate the relative safety of the tested compound on normal cells.

Table 4. Antiproliferative **IC_{50}± SEM (µM)** activity of compound **6l** and gefitinib

Sample code	M.W g/mol	Cytotoxicity IC_{50}± SEM (µM)	
		RPMI-8226	**WI38**
6l	315.06	15.72±1.21	46.05±2.36
Gefitinib	446.90	9.92±0.62	33.49±1.73

2.2.4. EGFR TK Inhibitory Activity

Epidermal growth factor receptor (EGFR) and its mediated signaling pathway regulate many physiological processes such as cell growth, proliferation and differentiation In recent years, EGFR has become a hot therapeutic target for cancer. The mechanism at molecular level of the selected most active antiproliferative compound **6l** was investigated on mutant and wild EGFR TK kinase (**Table 5**) [33]. The findings of the cancer cell-based assays have been powerfully complemented by the results from EGFR assay. Compound **6l** showed moderated EGFR inhibition with IC_{50}= 695.49±21.8 and 263.15±15.13 nM on the mutant and wild EGFR respectively, while that of gefitinib was 358.78±17.2 and 157.54±4.85 nM.

Table 5. EGFR-TK Inhibitory activity of compounds **6l** and gefitinib.

Compound	EGFR IC_{50} nM	EGFR-T490M IC_{50} nM
6l	695.49±21.8	263.15±15.13
Gefitinib	358.78±17.2	157.54±4.85

2.2.5. Human RAS Inhibitory Activity

Ras proteins are among the most frequently mutated drivers in human cancer and the quest for compounds that bind to mutant RAS remains a major goal as elusive anti-cancer pharmaceutical

targeting A [34]. Mutations in the RAS family of proto-oncogenes (comprising H-RAS, N-RAS and K-RAS) are very common, being found in 20% to 30% of all human tumors [35,36]. It is reasonable to speculate that a pharmacological approach that curtails RAS activity may represent a possible method to inhibit certain cancer types [37].

Compound **6l** has been investigated on RPMI-8226 leukemia cell line as a possible H-RAS inhibitor, using gefitinib as reference. The results showed that **6l** achieved good activity with 10.61±0.27 ng/ml against gefitinib with 7.688±0.23 ng/ml on the same cell line (**Table 6** and **Figure 3**).

Table 6. RAS and **STAT3** inhibitory activities of compounds **6l** and gefitinib

Compound	H-RAS conc. ng/ml	STAT3 conc. ng/ml
6l/RPMI-8226	10.61±0.27	1.753±0.81
Gefitinib/RPMI-8226	7.688±0.23	1.28±0.04
Cont.RPMI-8226	21.75±1.71	3.73±0.07

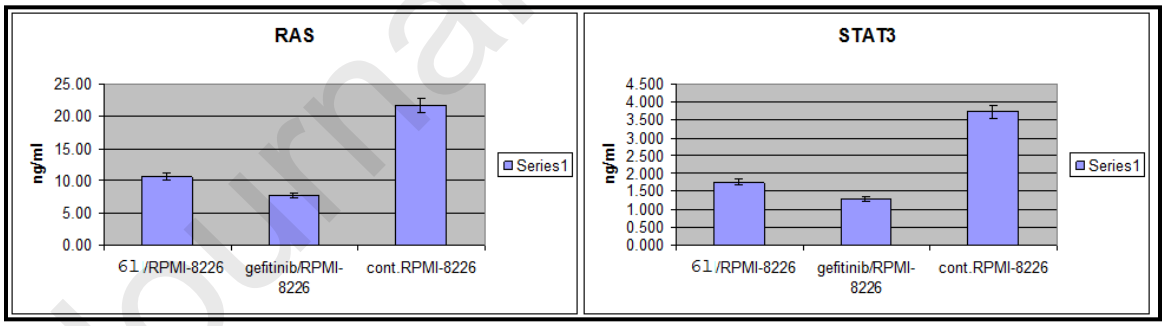

Figure 3. RAS and **STAT3** inhibitory activities of compounds **6l** and gefitinib

2.2.6. STAT3 Inhibitory Activity

STAT proteins also known as Signal Transducer and Activator of Transcription are transcription factors involved in a huge repertoire of biological signal transduction cascades leading to embryonic development, programmed cell death, organogenesis, innate immunity, adaptive

immunity and cell growth regulation in organisms ranging from insects to man [38]. There are seven mammalian STAT family members that have been identified: STAT1, 2, 3, 4, 5 and 6. STAT proteins are thought to be ideal targets for anti-cancer therapy since cancer cells are more dependent on the STAT activity than their normal counterparts [39,40]. Compound **6l** has been investigated on RPMI-8226 leukemia cell line as a possible STAT3 inhibitor, using gefitinib as reference. The results showed that **6l** achieved excellent activity with result 1.753±0.81 ng/ml comparable to gefitinib with 1.28±0.04 ng/ml on leukemia cell line (**Table 6** and **Figure 3**).

2.2.7. Activation of caspases cascade

Activation of caspases plays a key role in the initiation and effecting of the apoptotic process [41]. Among the most common caspases, caspase-3 is an essential player that cleaves multiple proteins in the cells, leading to apoptotic cell death [42]. The effect of compound **6l** on caspase 3 was evaluated and compared to gefitinib as a reference drug on RPMI-8226 cell line. Compound **6l** showed an increase in the level of active caspase 3 by 5.31-fold compared to gefitinib (4.58-fold) as shown in **Table 7**. Moreover, effect of compound **6l** on caspase 8 was also evaluated; compound **6l** increases the levels of caspase-8 by 1.54-fold, while gefitinib was 1.85-fold. The data indicate that **6l** is potential activators of both intrinsic and extrinsic caspase.

Table 7. Effect of compound **6l** and gefitinib on the active caspases-3 and 8 in RPMI-8226 cell line.

Comp. Number	Caspase-3		Caspase-8	
	Conc (ng/ml)	Fold change	Conc (ng/ml)	Fold change
6l	322.7±14.7	5.31	0.5475±0.03	1.546173
Gefitinib	278.6±15.1	4.58	0.6581±0.09	1.858515
Control	60.76±4.02	1	0.3541±0.02	1

2.2.8. Effects on BAX and Bcl-2 proteins

Bcl-2 (B-cell lymphoma 2) family members are significant regulators of apoptosis that can be classified into three groups. The first group protects against apoptosis (Bcl-2 itself), the second group of proteins is represented by Bax (Bcl-2 associated protein X) and Bak (Bcl-2 antagonist/killer). Bax and Bak are the key activators of the apoptosis machinery in response to cellular stress stimuli. The third group is comprised of different categories of proteins such as Bid (BH3 interacting death domain), Bim (Bcl-2 interacting mediator) and others [43] .Overexpression of the antiapoptotic Bcl-2 members leading to antagonizing apoptosis and development of resistance of tumor cells to common chemotherapeutic agents. Thus, the development of new drugs that can inhibit the action of antiapoptotic Bcl-2 members is very attractive strategy in design of anticancer agents [44]. The effect of compound **6l** on the expression levels of Bcl2 and BAX was determined after treatment of RPMI-8226 cell line with the IC_{50} of compound **6l** and the results were illustrated in **Table 8**. Compound **6l** caused up-regulation in the level of the proapoptotic protein BAX by approximately 6.5 folds while it markedly down-regulated the levels of the antiapoptotic proteins Bcl2 up to 0.4 folds compared to the control untreated cells. These findings proved the proapoptotic effect of compound **6l.**

Table 8. Bax and Bcl-2 levels for compounds **6l** and gefitinib on **RPMI-8226** cell line**.**

Compound	**Bax**		**Bcl-2**	
	Conc (pg/ml)	Fold change	Conc (ng/ml)	Fold change
6l	239.7±9.61	6.543221	3.29±0.14	0.486471
Gefitinib	309.6±11.8	8.451319	3.747±0.22	0.554044
Control	36.63±1.96	1	6.763±0.46	1

2.2.9. Cell cycle analysis and apoptosis assay

2.2.9.1. Cell cycle analysis

The cell cycle includes four phases: The G1 phase where cell enlargement and preparation of DNA duplication occurs; the S phase (synthesis) is the stage of DNA replication and chromatid duplication; in G2 Phase, repairing of new DNA and more growth occurs while in the M stage nuclear division takes place. Studies on the effect of compound **6l** on cell cycle development and induction of apoptosis in the RPMI-8226 were done. RPMI-8226 was incubated with IC_{50} concentration of compound **6l** for 24 h. Consequently, the cell line was stained with PI/Annexin V and analyzed by flow cytometry using BD FASCC alibur [45]. Investigation of the results in **Figure 4**, exposed that percentage of pre G1 apoptosis induced by **6l** on RPMI-8226 was 22.81%. A high percent of cell accumulation was observed in G2-M phase in RPMI-8226 treated with compound **6l** after 24 h incubation indicating arrest of cell cycle at G2-M phase.

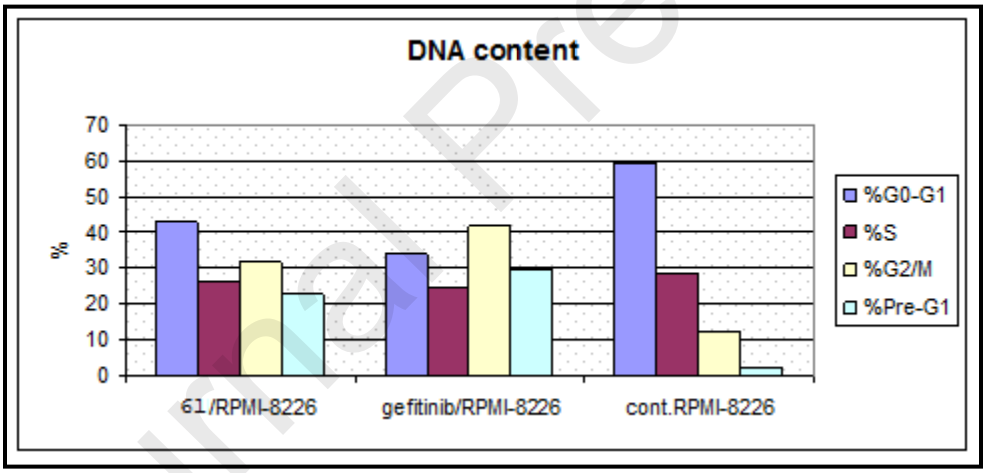

Figure 4. Cell cycle analysis results for compound **6l**

2.2.9.2. Apoptosis assay

Cell cycle analysis of RPMI-8226 after treatment with compound **6l** showed presence of pre-G1 peak which is an indication of apoptosis. To confirm the ability of **6l** to induce apoptosis, cells were stained with Annexin V/PI, incubated for 24 h and analyzed. Analysis of early and late apoptosis showed that compound **6l** was able to induce significant levels of apoptosis percent

3.61 and 17.45, respectively (Figures 5 and 6) and that % of necrosis was 1.75, while the reference gefitinib achieved 7.58 and 19.5 in apoptosis with 2.44 necrotic percentage.

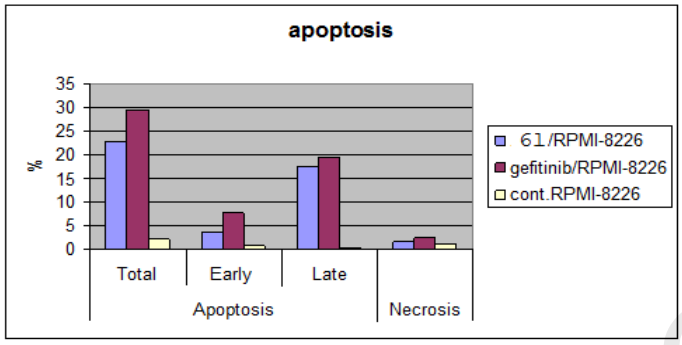

Figure 5. Apoptosis induction analysis using Annexin V/PI for compound **6l** and gefitinib

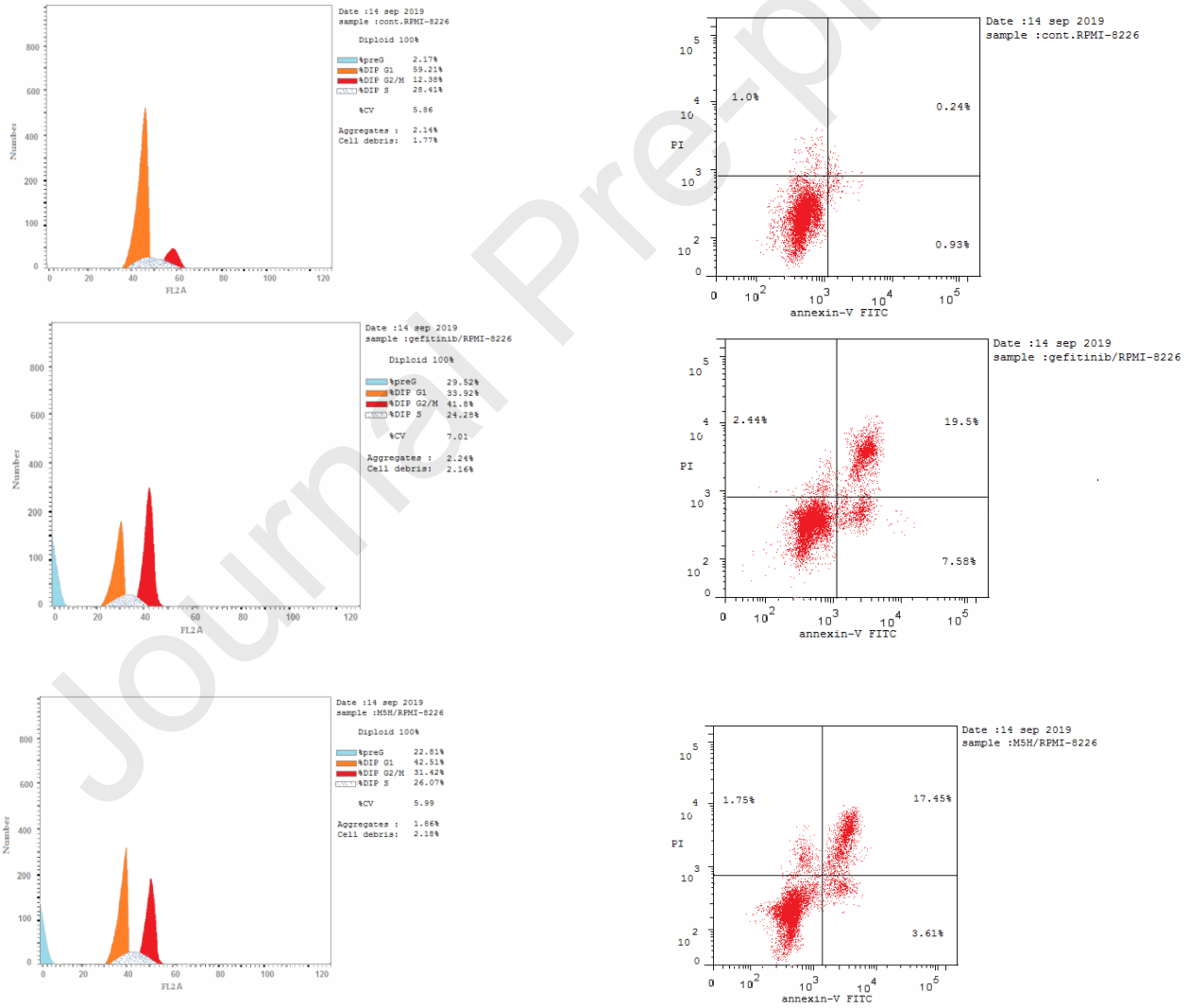

Figure 6. Apoptosis induction analysis using Annexin V/PI for compound **6l.**

2.3. Docking study

The target compounds were docked with EGFR receptor which are cocrystallized standard ligand gefitinib (ID: 2ITO) [46] extracted from protein data bank (PDB) using OpenEye scientific software [47-49]. The standard gefitinib was docked in a similar mode as its reported cocrystalized pose keeping the most important key interactions. Compound **6l** interacts with the receptor through formation of hydrogen bond (HB) with SER: 719: A (**Figure 7A**). Meanwhile this compound overlay with gefitinib and erlotinib standards inside the receptor (**Figures 7B**, **7C**) respectively with keeping. Meanwhile, the analogues compound 6c docked with EGFR receptor without illustrating any HB interactions (**Figure 7D**). It's clear that the kind of substitution on aryl group or quinolone moiety effects on compounds binding mode and pose which could give insight about the activity. In case of compounds **6a**, **6g**, **6d**, and **6m** docked with the receptor with weak interactions without formation of HB. Compounds **6o** and **6i** interacts with the receptor with formation of HBs with PHE 856: A, and THR 854: A respectively (**Appendix A**).

A

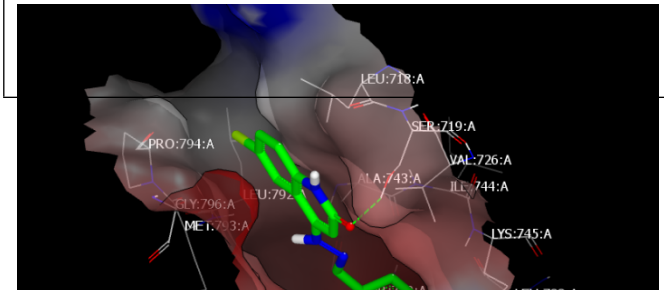

B

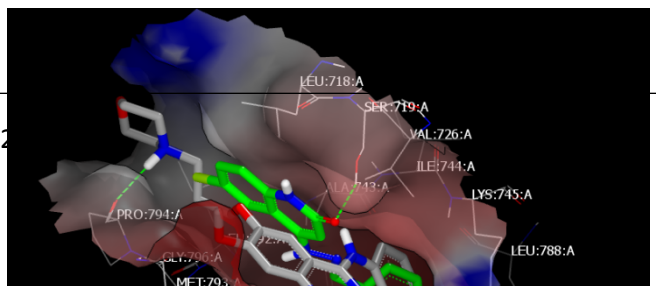

C 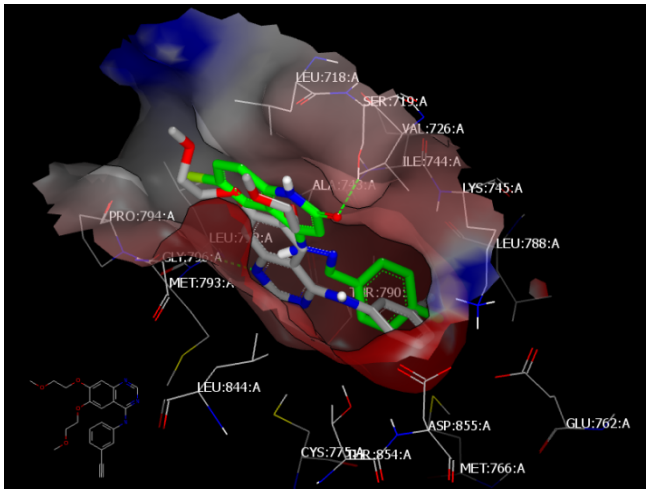	**D** 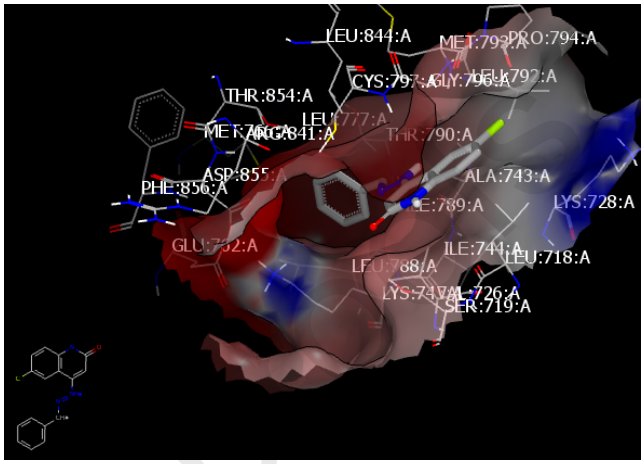

Figure 7: A) compound **6l** docked with EGFR receptor; B) compound **6l** with gefitinib in same receptor; C) compound **6l** with erlotinib in the receptor, D) compound **6c** docked without formation of HB interaction

In order to study the compound similarity to either gefitinib or erlotinib standards, the aim was directed to apply Rapid overlay chemical similarity analysis (ROCS) analysis. ROCS is a method that used to predict similarity between compounds based on their three dimensional [48]. Its alignment needs a) query molecules and here are erlotinib and gefitinib. b) The database molecules that our designed compounds especially compound **6l**. The outputs of ROC analysis are two forms: 1) the overlay between the query and database molecules as visualized by vROCS and VIDA applications [50]. The query will be visualized in term of shape counter, shape atoms, and color atoms labels.

The color shape of gefitinib showed the following atoms labels 4 rings, 2 donors, 5 acceptors and 1 cation site (**Figure 8A**). The color shape of erlotinib represented 3 rings, 1 donor, 6 acceptors and one hydrophobic site (**Figure 8B**). Compounds **6l** showed overlay with gefitinib, and

erlotinib as represented in **Figures 8C** and **8D**, respectively. According to these mapping, compound **6l** illustrated high similarity to erlotinib drug. From these visualizations we can be envisioned for elaboration a new derivative rom **6l** through installing side chain to benzene ring of quinoline-2-one moiety.

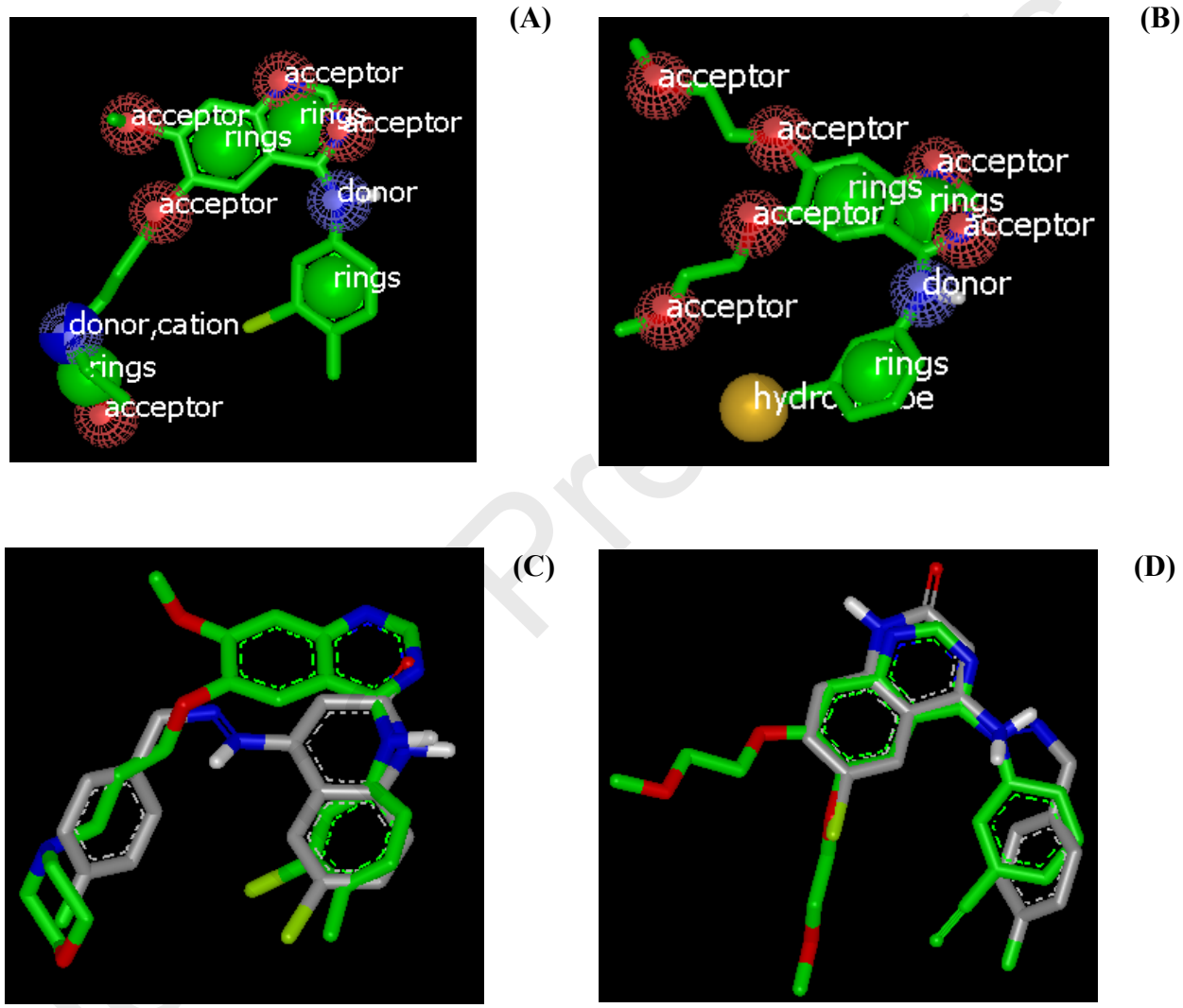

Figure 8. A) ROCS analysis overlay of gefitinib as query; B) erlotinib as query; C) **6l** with gefitinib; D) **6l** with erlotinib

The second output of ROCs analysis is the Tanimoto Combo (TC) score, table 9. TC score represents various aspects of that alignment. Tanimoto Combo is the sum of Shape Tanimoto

(Tanimoto coefficient) and Color Tanimoto scores. The scores are computed and the process is repeated to each conformation of the query molecules (gefitinib and erlotinib) and each conformation for the database molecule **6l** (**Table 9**). The target compound showed higher score in Tanimoto combo to lead erlotinib (0.84) rather than the gefitinib 0.76.

Table 9: Tanimoto combo score for compound **6l**, and lead compounds Erlotinib and Gefitinib as query

	Erlotinb (Tanimato combo)	**Gefitinb (Tanimato combo)**
Erlotinib	2	0.94
Gefitinib	0.96	2
6l	0.84	0.76

2.4. Structure activity relationship:

The final compounds have two variation sites either on position 6 of quinolin-one ring (R^1) or on para position of aryl hydrazine moiety (R^2) as represented in **Figure 1**.

Installing R^1 as electron withdrawal group (EWG) improved the activity of compounds rather than the corresponding unsubstituted or those with electron donating group (EDG) as showed in compound **6l** and **6f** versus compounds **6d**, and **6e**. In the same way, tethering the phenyl group of hydrazone moiety with R^2 as EWG increases the compounds activity. It was clear compounds with both R^1 and R^2 as EWGs have higher activity (compounds **6l** and **6f**). The maximum biological effect has gained in compound **6l** with chlorine and fluorine atom in both positions, achieving the highest results among all tested compounds with complete inhibition of the tested leukemia cancer cell lines, **Table 2.**

3. Conclusions

A series of new 2-quinolone-4-arylidene derivatives **6a-o** was prepared and characterized using different spectroscopic techniques. Some of the target compounds have promising anticancer

activities. The 6-chloro derivative **6l** was found to be the most active derivative among this series. It showed outstanding inhibition on all leukemia cell lines tested with mean GI_{50} of 14.94 according to NCI protocol. The IC50 was determined as 15.72±1.21 compared to gefatinib (9.92±0.62). Also, **6l** showed inhibitory activity with comparable potency to gefatinib against EGFR-TK mutant and wild cells. Similarly, **6l** have inhibitory activity against H.RAS and STAT-3 on leukemia cell lines. Moreover, **6l** increased the level of Caspase-3 by 1.54 folds compared to gefatinib (1.85) fold increase. Also, the effect of **6l** on apoptotic regulators, BAX and BCl-2 proved its proapoptotic effect. Results of cell cycle analysis showed that **6l** can accomplish cell cycle arrest at G2/M phas; **6l** can induce apoptosis when stained with Annexin V/PT. Results from molecular docking study showed that **6l** can overlay with gefatinib and erlotinib in binding to the protein (ID: 2ITO). The rapid overlay chemical similarity analysis (ROCS) of **6l** experienced similarity to erlotinib more than gefatinib in binding. Hence, **6l** is considered promising lead candidate erlotinib analogue effective in leukemia that require further optimization.

4. Experimental

4.1. Chemistry

All materials were obtained from commercial suppliers and used without further purification. Reactions were monitored by TLC (Kieselgel 60 F_{254}precoated plates, E. Merck, Germany), the spots were detected by exposure to UV lamp at 254 nm. Melting points were determined on an electro thermal melting point apparatus (Stuart Scientific Co.) and were uncorrected. NMR spectra were measured on a Bruker AV-400 spectrometer (Bruker Bio Spin Corp., Billerica, MA, USA) (400 MHz for ^{1}H, 101 MHz for ^{13}C) at Florida Institute of Technology, USA. The ^{1}H and ^{13}C chemical shifts are given relative to internal standard TMS = 0., and external liquid ammonia

= 0 for ^{15}N. Coupling constants are stated in Hz. Correlations were established using ^{1}H-^{1}H COSY, and ^{1}H-^{13}C and ^{1}H-^{15}N HSQC and HMBC experiments. Vario EL III German CHN Elemental analyzer model was used for Elemental analysis. Preparation and analytical data of compounds **2-5** were as reported in lit [28-30,31].

4.1.1. General synthesis of compounds **6a-o**

To a suspension of hydrazine- quinoline-2-one **5** (1.0 mmol) in ethanol (20 mL); an appropriate aryl aldehyde derivative (1.0 mmol) with 2 drops of glacial acetic acid were added. The reaction mixture was heated under reflux for 5-8 h. After cooling, the formed precipitate was filtered, washed with diethyl ether and crystallized from ethanol.

(*E*)-4-(2-Benzylidenehydrazinyl)quinolin-2(1*H*)-one (**6a**)

Yield: 0.22 g (85%); mp: 180–182 °C, ^{1}H NMR (400 MHz, DMSO-d_6) δ ppm 11.08 (s, 1H, O=C-NH), 10.79 (s, 1H, N-NH), 8.39 (s, 1H, N=CH), 8.05 (d, J = 8.1, 1H, quin-Ar-H), 7.75 (d, J = 7.3 Hz, 2H, Ar-H), 7.50 (t, J = 7.6 Hz, 1H, quin-Ar-H), 7.46 (t, J = 7.6 Hz, 2H , Ar-H), 7.41 (t, J = 7.1 Hz, 1H, Ar-H), 7.30 (d, J = 8.2 Hz, 1H, quin-Ar-H), 7.19 (t, J = 7.6 Hz, 1H, quin-Ar-H), 6.24 (s, 1H, C=CH).^{13}C NMR (101 MHz, DMSO-d_6) δ ppm 162.29, 147.88, 143.21, 138.91, 134.22, 129.93, 128.97, 128.38, 126.13, 121.43, 120.21, 115.23, 111.33, 93.75. LCMS: m/z calcd: 263.11, found $[M-H]^{-}$: 262.10. Anal. Calcd for $C_{16}H_{13}N_3O$ (263.11): C, 72.99; H, 4.88; N, 15.96. Found: C, 73.19; H, 4.66; N, 16.08.

(*E*)-4-(2-Benzylidenehydrazinyl)-6-methylquinolin-2(1*H*)-one (**6b**)

Yield: 0.23 g (83%); mp: 185–187 °C,^{1}H NMR (400 MHz, DMSO-d_6) δ ppm 11.09 (s, 1H, O=C-NH), 10.77 (s, 1H, N-NH), 8.39 (s, 1H, N=CH), 7.88 (s, 1H, quin-Ar-H), 7.74 (d, J = 7.4 Hz, 2H, Ar-H), 7.45 (t, J = 7.2 Hz, 2H , Ar-H), 7.39 (t, J = 7.1 Hz, 1H, Ar-H), 7.33 (d, J = 8.3 Hz, 1H, quin-Ar-H), 7.22 (d, J = 8.3 Hz, 1H, quin-Ar-H), 6.26 (s, 1H, C=CH), 2.38 (s, 3H, CH_3).^{13}C NMR (101 MHz, DMSO-d_6) δ ppm 162.34, 147.76, 143.06, 136.89, 134.25, 131.07, 129.93,

128.92, 128.36, 126.09, 120.96, 115.16, 111.24, 93.74, 20.20. LCMS: m/z calcd: 277.12, found [M-H]$^-$: 276.10. Anal. Calcd for $C_{17}H_{15}N_3O$ (277.12): C, 73.63; H, 5.45; N, 15.15. Found: C, 73.96; H, 5.23; N, 15.40.

(*E*)-4-(2-Benzylidenehydrazinyl)-6-chloroquinolin-2(1*H*)-one (**6c**)

Yield: 0.23 g (79%); mp: 191–193 °C, ^{1}H NMR (400 MHz, DMSO-d_6) δ ppm 10.78 (s, 1H, O=C-NH), 10.38 (s, 1H, N-NH), 7.91 (s, 1H, N=CH), 7.73 (s, 1H, quin-Ar-H), 7.29 (d, J = 7.2 Hz, 2H, Ar-H), 7.07 (d, J = 7.6 Hz, 1H, quin-Ar-H), 7.01-6.94 (m, 3H , Ar-H), 6.84 (d, J = 7.9 Hz, 1H, quin-Ar-H), 5.80 (s, 1H, C=CH). ^{13}C NMR (101 MHz, DMSO-d_6) δ ppm 162.07, 147.00, 143.58, 137.69, 134.07, 129.86, 129.08, 128.38, 126.20, 124.51, 120.92, 117.03, 112.54, 94.39. LCMS: m/z calcd: 297.07, found [M-H]$^-$: 296.00. Anal. Calcd for $C_{16}H_{12}ClN_3O$ (277.12): C, 64.54; H, 4.06; N, 14.11. Found: C, 64.63; H, 3.97; N, 14.04.

(*E*)-4-(2-(4-Methoxybenzylidene)hydrazinyl)quinolin-2(1*H*)-one (**6d**)

Yield: 0.21 g (73%); mp: 165-167 °C,^{1}H NMR (400 MHz, DMSO-d_6) δ ppm 10.60 (s, 1H, O=C-NH), 10.21 (s, 1H, N-NH), 7.90 (s, 1H, N=CH), 7.58 (d, J = 7.8, 1H, quin-Ar-H), 7.29 (d, J = 7.2 Hz, 2H, Ar-H), 7.04 (t, J = 7.4, 1H, quin-Ar-H), 6.83 (d, J = 8.2 Hz, 1H, quin-Ar-H), 6.73 (t, J = 7.6 Hz, 1H, quin-Ar-H), 6.57 (d, J = 7.6 Hz, 2H, Ar-H), 5.74 (s, 1H, C=CH), 3.34 (s, 3H, OCH_3).^{13}C NMR (101 MHz, DMSO-d_6) δ ppm 168.14, 165.62, 153.69, 148.96, 144.60, 135.57, 133.38, 132.53, 127.13, 125.88, 120.93, 119.57, 117.10, 98.91, 60.48. LCMS: m/z calcd: 293.12, found [M-H]$^-$: 292.10. Anal. Calcd for $C_{17}H_{15}N_3O_2$ (293.12): C, 69.61; H, 5.15; N, 14.33. Found: C, 69.40; H, 5.13; N, 14.52.

(*E*)-4-(2-(4-Mthoxybenzylidene)hydrazinyl)-6-methylquinolin-2(1*H*)-one **(6e**)

Yield: 0.21 g (70%); mp: 205–207 °C, ^{1}H NMR (400 MHz, DMSO-d_6) δ ppm 11.05 (s, 1H, O=C-NH), 10.63 (s, 1H, N-NH), 8.33 (s, 1H, N=CH), 7.86 (s, 1H, quin-Ar-H), 7.68 (d, J = 7.8

Hz, 2H, Ar-H), 7.32 (d, *J* = 8.1 Hz, 1H, quin-Ar-H), 7.21 (d, *J* = 8.3 Hz, 1H, quin-Ar-H), 7.45 (d, *J* = 7.6 Hz, 2H , Ar-H), 6.22 (s, 1H, C=CH), 3.36 (s, 3H, OCH_3), 2.36 (s, 3H, CH_3).^{13}C NMR (101 MHz, DMSO-d_6) δ ppm 162.42, 15.88, 147.83, 143.09, 136.87, 131.09, 129.16, 127.64, 126.87, 120.95, 115.18, 113.85, 111.28, 93.22, 54.73, 20.19. LCMS: m/z calcd: 307.13, found [M-H]$^-$: 306.10. Anal. Calcd for $C_{18}H_{17}N_3O_2$ (307.13): C, 70.34; H, 5.58; N, 13.67. Found: C, 70.01; H, 5.78; N, 13.48.

(*E*)-6-Chloro-4-(2-(4-methoxybenzylidene)hydrazinyl)quinolin-2(1*H*)-one (**6f**).

Yield: 0.30 g (93%); mp: 212–214 °C,^{1}H NMR (400 MHz, DMSO-d_6) δ ppm 10.74 (s, 1H, O=C-NH), 10.22 (s, 1H, N-NH), 7.85 (s, 1H, N=CH), 7.72 (s, 1H, quin-Ar-H), 7.24 (d, *J* = 8.0 Hz, 2H, Ar-H), 7.09 (d, *J* = 7.8 Hz, 1H, quin-Ar-H), 6.83 (d, *J* = 8.1 Hz, 1H, quin-Ar-H), 6.55 (d, *J* = 8.1 Hz, 2H , Ar-H), 5.77 (s, 1H, C=CH), 3.34 (s, 3H, OCH_3).^{13}C NMR (101 MHz, DMSO-d_6) δ ppm 162.14, 159.99, 147.05, 143.59, 137.67, 129.77, 127.76, 126.68, 124.46, 120.90, 117.00, 113.86, 112.59, 93.85, 54.78. LCMS: m/z calcd: 327.08, found [M-H]$^-$: 326.00. Anal. Calcd for $C_{17}H_{14}ClN_3O_2$ (327.08): C, 62.30; H, 4.31; N, 12.82. Found: C, 62.18; H, 4.35; N, 12.64.

(*E*)-4-(2-(4-(Dimethylamino)benzylidene)hydrazinyl)quinolin-2(1*H*)-one (**6g**)

Yield: 0.27 g (89%); mp: 228-230 °C,^{1}H NMR (400 MHz, DMSO-d_6) δ ppm 10.95 (s, 1H, O=C-NH), 10.47 (s, 1H, N-NH), 8.28 (s, 1H, N=CH), 8.04 (d, *J* = 7.8 Hz, 1H, quin-Ar-H), 7.57 (d, *J* = 7.2 Hz, 2H, Ar-H), 7.48 (t, *J* = 7.4 Hz, 1H, quin-Ar-H), 7.28 (d, *J* = 8.2 Hz, 1H, quin-Ar-H), 7.18 (t, *J* = 7.6 Hz, 1H, quin-Ar-H), 6.78 (d, *J* = 7.6 Hz, 2H , Ar-H), 6.15 (s, 1H, C=CH), 2.98 (s, 6H, $N(CH_3)_2$).^{13}C NMR (101 MHz, DMSO-d_6) δ ppm 162.85, 151.16, 148.37, 144.78, 139.36, 130.18, 127.89, 122.15, 121.86, 120.50, 115.62, 111.94, 93.12, 39.51. LCMS: m/z calcd: 306.15,

found [M-H]$^-$: 305.10. Anal. Calcd for $C_{18}H_{18}N_4O$ (306.15): C, 69.61; H, 5.15; N, 14.03. Found: C, 69.30; H, 5.13; N, 13.92.

(*E*)-4-(2-(4-(Dimethylamino)benzylidene)hydrazinyl)-6-methylquinolin-2(1*H*)-one (**6h**)

Yield: 0.27 g (87%); mp: 176–178 °C,^{1}H NMR (400 MHz, DMSO-d_6) δ ppm 10.89 (s, 1H, O=C-NH), 10.42 (s, 1H, N-NH), 8.26 (s, 1H, N=CH), 7.85 (s, 1H, quin-Ar-H), 7.56 (d, J = 8.8 Hz, 2H, Ar-H), 7.31 (d, J = 8.4 Hz, 1H, quin-Ar-H), 7.18 (d, J = 8.3 Hz, 1H, quin-Ar-H), 6.77 (d, J = 7.6 Hz, 2H , Ar-H), 6.14 (s, 1H, C=CH), 2.98 (s, 6H, $N(CH_3)_2$), 2.38 (s, 3H, CH_3).^{13}C NMR (101 MHz, DMSO-d_6) δ ppm 162.80, 151.14, 148.18, 144.60, 137.34, 131.31, 129.45, 127.85, 122.20, 121.38, 115.53, 111.94, 111.79, 93.17, 39.78, 20.64. LCMS: m/z calcd: 320.16, found [M-H]$^-$: 319.10. Anal. Calcd for $C_{19}H_{20}N_4O$ (320.16): C, 71.23; H, 6.29; N, 17.49. Found: C, 71.47; H, 6.13; N, 17.27.

(*E*)-6-Chloro-4-(2-(4-(Dimethylamino)benzylidene)hydrazinyl)quinolin-2(1*H*)-one (**6i**).

Yield: 0.28 g (83%); mp: 210–212 °C,^{1}H NMR (400 MHz, DMSO-d_6) δ ppm 11.10 (s, 1H, O=C-NH), 10.52 (s, 1H, N-NH), 8.25 (s, 1H, N=CH), 8.18 (d, J = 2.0 Hz, 1H, quin-Ar-H), 7.57 (d, J = 8.8 Hz, 2H, Ar-H), 7.54 (dd, J = 8.9,2.1 Hz, 1H, quin-Ar-H), 7.29 (d, J = 8.8 Hz, 1H, quin-Ar-H), 6.77 (d, J = 8.8 Hz, 2H, Ar-H), 6.17 (s, 1H, C=CH), 2.98 (s, 6H, $N(CH_3)_2$).^{13}C NMR (101 MHz, DMSO-d_6) δ ppm 162.63, 151.24, 147.48, 145.15, 138.15, 130.11, 127.97, 124.83, 121.99, 121.35, 117.42, 113.15, 111.91, 93.74, 39.57. LCMS: m/z calcd: 340.11, found [M-H]$^-$: 339.20. Anal. Calcd for $C_{18}H_{17}ClN_4O$ (340.11): C, 63.44; H, 5.03; N, 16.44. Found: C, 63.62; H, 4.99; N, 16.27.

(*E*)-4-(2-(4-Fluorobenzylidene)hydrazinyl)quinolin-2(1*H*)-one (**6j**).

Yield: 0.26 g (95%); mp: 211-213 °C,^{1}H NMR (400 MHz, DMSO-d_6) δ ppm 11.17 (s, 1H, O=C-NH), 10.83 (s, 1H, N-NH), 8.38 (s, 1H, N=CH), 8.06 (d, J = 8.1 Hz, 1H, quin-Ar-H), 7.80 (dd, J = 7.7, 6.0 Hz, 2H, Ar-H), 7.50 (t, J = 7.6 Hz, 1H, quin-Ar-H), 7.30 (dd, J = 11.9, 8.5 Hz, 2H ,

Ar-H),7.26 (d, *J* = 8.6 Hz, 1H, quin-Ar-H), 7.18 (t, *J* = 7.5 Hz, 1H, quin-Ar-H), 6.27 (s, 1H, C=CH). ^{13}C NMR (101 MHz, DMSO-d_6) δ ppm 162.42, 162.25, 147.95, 142.08, 138.89, 130.82, 129.93, 128.20, 121.43, 120.24, 115.37, 115.26, 111.35, 93.71. LCMS: m/z calcd: 281.10, found [M-H]$^-$: 280.10. Anal. Calcd for $C_{16}H_{12}FN_3O$ (281.10): C, 68.32; H, 4.30; N, 14.94. Found: C, 68.50; H, 4.16; N, 15.11.

(*E*)-4-(2-(4-Fluorobenzylidene)hydrazinyl)-6-methylquinolin-2(1*H*)-one (**6k**)

Yield: 0.24 g (83%); mp: 169-171 °C, ^{1}H NMR (400 MHz, DMSO-d_6) δ ppm 10.62 (s, 1H, O=C-NH), 10.31 (s, 1H, N-NH), 7.92 (s, 1H, N=CH), 7.40 (s, 1H, quin-Ar-H), 7.33 (d, *J* = 8.0 Hz, 1H, quin-Ar-H), 6.84 (d, *J* = 7.8 Hz, 2H, Ar-H), 6.80 (d, *J* = 8.0 Hz, 1H, quin-Ar-H), 6.76 (d, *J* = 7.8 Hz, 2H , Ar-H), 5.79 (s, 1H, C=CH), 1.91 (s, 3H, CH_3).^{13}C NMR (101 MHz, DMSO-d_6) δ ppm 163.45, 162.36, 160.99, 147.76, 141.89, 136.87, 131.05, 130.88, 129.21, 128.11, 120.94, 115.46, 115.24, 115.15, 111.23, 93.73, 20.18. LCMS: m/z calcd: 295.11, found [M+H]$^+$: 296.00. Anal. Calcd for $C_{17}H_{14}FN_3O$ (295.11): C, 69.14; H, 4.78; N, 14.23. Found: C, 68.95; H, 4.51; N, 14.18.

(*E*)-6-Chloro-4-(2-(4-fluorobenzylidene)hydrazinyl)quinolin-2(1*H*)-one (**6l**).

Yield: 0.25 g (80%); mp: 178-180 °C ^{1}H NMR (400 MHz, DMSO-d_6) δ ppm 11.28 (s, 1H, O=C-NH), 10.82 (s, 1H, N-NH), 8.32 (s, 1H, N=CH), 8.16 (s, 1H, quin-Ar-H), 7.77 (d, *J* = 8.2 Hz, 1H, quin-Ar-H), 7.52 (d, *J* = 8.0 Hz, 2H, Ar-H), 7.31 (d, *J* = 8.1 Hz, 1H, quin-Ar-H), 7.25 (d, *J* = 7.8 Hz, 2H , Ar-H), 6.28 (s, 1H, C=CH).^{13}C NMR (101 MHz, DMSO-d_6) δ ppm 163.54, 162.18, 161.07, 147.04, 142.39, 137.62, 130.71, 129.83, 128.30, 124.52, 120.92, 117.03, 115.49, 115.27, 112.55, 94.41. LCMS: m/z calcd: 315.06, found [M-H]$^-$: 314.00. Anal. Calcd for $C_{16}H_{11}ClFN_3O$ (315.06): C, 60.87; H, 3.51; N, 13.31. Found: C, 60.72; H, 3.69; N, 13.17.

(*E*)-4-(2-(4-Chlorobenzylidene)hydrazinyl)quinolin-2(1*H*)-one (**6m**)

Yield: 0.27 g (91%); mp: 213-215 °C,^{1}H NMR (400 MHz, DMSO-d_6) δ ppm 11.11 (s, 1H, O=C-NH), 10.86 (s, 1H, N-NH), 8.36 (s, 1H, N=CH), 8.04 (d, J = 8.2 Hz, 1H, quin-Ar-H), 7.78 (d, J = 8.4 Hz, 2H, Ar-H), 7.51 (d, J = 8.3 Hz, 2H , Ar-H), 7.50 (t, J = 7.6 Hz, 1H, quin-Ar-H), 7.30 (d, J = 8.2 Hz, 1H, quin-Ar-H), 7.19 (t, J = 7.6 Hz, 1H, quin-Ar-H), 6.25 (s, 1H, C=CH).^{13}C NMR (101 MHz, DMSO-d_6) δ ppm 162.27, 147.79, 141.81, 138.90, 133.28, 133.18, 129.97, 128.43, 127.74, 121.42, 120.24, 115.24, 111.30, 93.98. LCMS: m/z calcd: 297.07, found [M-H]$^-$: 296.10. Anal. Calcd for $C_{16}H_{12}ClN_3O$ (297.07): C, 64.54; H, 4.06; N, 14.11. Found: C, 64.72; H, 4.06; N, 14.37.

(*E*)-4-(2-(4-Chlorobenzylidene)hydrazinyl)-6-methylquinolin-2(1*H*)-one (**6n**).

Yield: 0.23 g (77%); mp: 160-162 °C, ^{1}H NMR (400 MHz, DMSO-d_6) δ ppm 11.04 (s, 1H, O=C-NH), 10.80 (s, 1H, N-NH), 8.36 (s, 1H, N=CH), 7.85 (s, 1H, quin-Ar-H), 7.77 (d, J = 8.5 Hz, 2H, Ar-H), 7.50 (d, J = 8.4 Hz, 2H , Ar-H), 7.33 (d, J = 8.3 Hz, 1H, quin-Ar-H), 7.20 (d, J = 8.0 Hz, 1H, quin-Ar-H), 6.23 (s, 1H, C=CH), 2.38 (s, 3H, CH_3).^{13}C NMR (101 MHz, DMSO-d_6) δ ppm 162.20, 147.58, 141.62, 136.89, 133.23, 133.21, 131.09, 129.21, 128.43, 127.70, 120.92, 115.14, 111.18, 94.02, 20.20. LCMS: m/z calcd: 311.08, found [M-H]$^-$: 310.00. Anal. Calcd for $C_{17}H_{14}ClN_3O$ (311.08): C, 65.49; H, 4.53; N, 13.48. Found: C, 65.24; H, 4.71; N, 13.55.

(E)-6-Chloro-4-(2-(4-chlorobenzylidene)hydrazinyl)quinolin-2(1*H*)-one (**6o**).

Yield: 0.25 g (77%); mp: 188-190 °C ^{1}H NMR (400 MHz, DMSO-d_6) δ ppm 11.23 (s, 1H, O=C-NH), 10.88 (s, 1H, N-NH), 8.34 (s, 1H, N=CH), 8.18 (s, 1H, quin-Ar-H), 7.78 (d, J = 8.0 Hz, 2H, Ar-H), 7.55 (d, J = 8.5 Hz, 1H, quin-Ar-H), 7.51 (d, J = 7.8 Hz, 2H, Ar-H), 7.30 (d, J = 8.8 Hz, 1H, quin-Ar-H), 6.26 (s, 1H, C=CH). LCMS: m/z calcd: 331.03, found [M-H]$^-$: 330.00. Anal. Calcd for $C_{16}H_{11}Cl_2N_3O$ (331.03): C, 57.85; H, 3.34; N, 12.65. Found: C, 58.00; H, 3.39; N, 12.75.

4.2. Biological evaluation

4.2.1. NCI screening assay

As mentioned, the methodology of the NCI procedure for primary anticancer assay was detailed on their site (http://www.dtp.nci.nih.gov). But briefly, the protocol performed at sixty human tumor cell lines panel derived from different nine neoplastic diseases. NCI-60 testing is performed in two parts: first, a single concentration is tested in all 60 cell lines at a single dose of 10^{-5} molar or 15 µg/ml in accordance with the protocol of the Drug Evaluation Branch, National Cancer Institute, Bethesda, USA. If the results obtained meet selection criteria, then the compound is tested again in all 60 cell lines in 5 x 10 folds of dilution with the top dose being 10^{-4} molar or 150 µg/ml. Detailed methods are described in supplementary material related to this article.

4.2.2. MTT assay for cell viability

To investigate the effect of the newly synthesized compounds on leukemia cancer cells; MTT assay was performed against RPMI-8226 cell lines [31] **(See Appendix A)**.

4.2.3. EGFR inhibitory assay

EGFR assay was performed by established reported method using mutant and wild enzymes for selected synthetic compounds **6l**. Details are summarized in **Appendix A.**

4.2.4. Human RAS Inhibitory Activity

H-RAS assay was performed by established metod using (ELISA, Life Span Bio Sciences, Inco. Catalog No. LS-F16779) for **6l.** Details are summarized in **Appendix A.**

4.2.5. STAT3 Inhibitory Activity

STAT3 (Human) assay was performed on **6l** by (ELISA Kit , Bio Vision, Inco. Catalog # K4201-100), **Appendix A.**

4.2.6. Cell cycle analysis and apoptotic assay

4.2.6.1. Cell apoptosis and apoptotic detection

Studies on the effect of compound **6l** on cell cycle development and induction of apoptosis in the RPMI-8226 cell was done using the Annexin V-FITC Apoptosis Detection Kit (BioVision Research Products, USA). For more details see **Appendix A**.

4.2.6.2 Activation of Caspases

For more deeply and systematically investigation on cell apoptosis, the effect of compound **6l** on caspases-3 and 8 was evaluated and compared to gefitinib as a reference drug, details are summarized in **appendix A.**

4.2.6.3. Effects on BAX and Bcl-2 proteins.

The activities of compound **6l** against Bcl2 and BAX using RPMI-8226 cell cell line and gefitinib as a reference was investigated according to literature. **See Appendix A.**

4.2.7. Molecular modeling

4.2.7.1. Molecular docking study

The docking studies were performed using the OpenEye Modeling software, for more details see **Appendix A.**

4.2.7.2. Shape alignment and ROCS

Basic method to represent shape and color features in ROCS is using ROCs application Open Eye scientific software according to our previous studies*.

Acknowledgments

The authors thank the Deutsche Forschungsgemeinschaft (DFG) for their financial support of the accommodation of Prof Aly during his staying at the Karlsruhe Institute of Technology, Karlsruhe, Germany during the period of July/August 2019. Dr. Yaseen Elshaier, on behalf of

authors acknowledges the OpenEye Scientific Software Inc. (Santa Fe, NM, USA) for providing the academic license that helped in performing the docking and ROCS studies.

5. References

[1] S.M. Prajapati, K.D. Patel, R.H. Vekariya, S.N. Panchal, H.D. Patel, Recent advances in the synthesis of quinolines: a review, Rsc Advances, 4 (2014) 24463-24476.
[2] O. Navneetha, K. Deepthi, A.M. Rao, T.S. Jyostna, A review on chemotherapeutic activities of quinoline, International Journal of Pharmaceutical, Chemical & Biological Sciences, 7 (2017) 364–372.
[3] F. Barlési, C. Tchouhadjian, C. Doddoli, P. Villani, L. Greillier, J.P. Kleisbauer, P. Thomas, P. Astoul, Gefitinib (ZD1839, Iressa®) in non-small-cell lung cancer: A review of clinical trials from a daily practice perspective, Fundamental & clinical pharmacology, 19 (2005) 385-393.
[4] R. Iyer, A. Bharthuar, A review of erlotinib–an oral, selective epidermal growth factor receptor tyrosine kinase inhibitor, Expert opinion on pharmacotherapy, 11 (2010) 311-320.
[5] B. Bao, C. Mitrea, P. Wijesinghe, L. Marchetti, E. Girsch, R.L. Farr, J.L. Boerner, R. Mohammad, G. Dyson, S.R. Terlecky, Treating triple negative breast cancer cells with erlotinib plus a select antioxidant overcomes drug resistance by targeting cancer cell heterogeneity, Scientific reports, 7 (2017) 44125.
[6] A.C. Anderson, The Process of Structure-Based Drug Design, Chemistry & Biology, 10 (2003) 787-797.
[7] G. Klebe, Optimization of lead structures, Drug Design: Methodology, Concepts, and Mode-of-Action, (2013) 153-172.
[8] H. Zhao, Scaffold selection and scaffold hopping in lead generation: A medicinal chemistry perspective, Drug discovery today, 12 (2007) 149-155.
[9] B. Banerji, S.K. Killi, A. Katarkar, S. Chatterjee, Y. Tangella, C. Prodhan, K. Chaudhuri, Neo-tanshinlactone D-ring modified novel analogues induce apoptosis in human breast cancer cell via DNA damage, Bioorganic & medicinal chemistry, 25 (2017) 202-212.
[10] W.-B. Kuang, R.-Z. Huang, J.-L. Qin, X. Lu, Q.-P. Qin, B.-Q. Zou, Z.-F. Chen, H. Liang, Y. Zhang, Design, synthesis and pharmacological evaluation of new 3-(1H-benzimidazol-2-yl) quinolin-2 (1H)-one derivatives as potential antitumor agents, European journal of medicinal chemistry, 157 (2018) 139-150.
[11] M.A. Elbastawesy, A.A. Aly, M. Ramadan, Y.A. Elshaier, B.G. Youssif, A.B. Brown, G.E.-D.A. Abuo-Rahma, Novel Pyrazoloquinolin-2-ones: Design, Synthesis, Docking Studies, and Biological Evaluation as Antiproliferative EGFR-TK Inhibitors, Bioorganic chemistry, (2019) 103045.
[12] W.S. Hamama, A.E. Hassanien, M.G. El-Fedawy, H.H. Zoorob, Synthesis, PM3-Semiempirical, and Biological Evaluation of Pyrazolo [4, 3-c] quinolinones, Journal of Heterocyclic Chemistry, 53 (2016) 945-952.
[13] N.A. Taş, A. Şenocak, A. Aydın, Preparation and anticancer activities of some amino acid methyl ester schiff bases, Journal of the Turkish Chemical Society, 5 (2018) 585-606.
[14] N. Uddin, F. Rashid, S. Ali, S.A. Tirmizi, I. Ahmad, S. Zaib, M. Zubair, P.L. Diaconescu, M.N. Tahir, J. Iqbal, Synthesis, characterization, and anticancer activity of Schiff bases, Journal of Biomolecular Structure and Dynamics, 1 (2019) 1-14.

[15] S. Basu, A. Ganguly, P. Chakraborty, R. Sen, K. Banerjee, M. Chatterjee, T. Efferth, S.K. Choudhuri, Targeting the mitochondrial pathway to induce apoptosis/necrosis through ROS by a newly developed Schiff's base to overcome MDR in cancer, Biochimie, 94 (2012) 166-183.
[16] T. Kirubel Teshome, T. Tilahun Wubalem, Schiff Bases and their metal complexes as potential anticancer candidates: A review of recent works, Anti-Cancer Agents in Medicinal Chemistry, 19 (2019) 1-10.
[17] K.M. Khan, U. Salar, S. Afzal, A. Wadood, M. Taha, S. Perveen, H. Khan, J. Lecka, J. Sévigny, J. Iqbal, Schiff bases of tryptamine as potent inhibitors of nucleoside triphosphate diphosphohydrolases (NTPDases): Structure-activity relationship, Bioorganic chemistry, 82 (2019) 253-266.
[18] S. Ambika, Y. Manojkumar, S. Arunachalam, B. Gowdhami, K.K.M. Sundaram, R.V. Solomon, P. Venuvanalingam, M.A. Akbarsha, M. Sundararaman, Biomolecular interaction, anti-cancer and anti-angiogenic properties of cobalt (III) Schiff base complexes, Scientific reports, 9 (2019) 2721.
[19] S. Adsule, V. Barve, D. Chen, F. Ahmed, Q.P. Dou, S. Padhye, F.H. Sarkar, Novel Schiff base copper complexes of quinoline-2 carboxaldehyde as proteasome inhibitors in human prostate cancer cells, Journal of medicinal chemistry, 49 (2006) 7242-7246.
[20] S. Demirci, A. Doğan, N. Başak, D. Telci, B. Dede, C. Orhan, M. Tuzcu, K. Şahin, N. Şahin, I.H. Özercan, A Schiff base derivative for effective treatment of diethylnitrosamine-induced liver cancer in vivo, Anti-cancer drugs, 26 (2015) 555-564.
[21] K.O. Alfarouk, C.-M. Stock, S. Taylor, M. Walsh, A.K. Muddathir, D. Verduzco, A.H. Bashir, O.Y. Mohammed, G.O. Elhassan, S. Harguindey, Resistance to cancer chemotherapy: failure in drug response from ADME to P-gp, Cancer cell international, 15 (2015) 71.
[22] R. O'Connor, M. Clynes, P. Dowling, N. O'Donovan, L. O'Driscoll, Drug resistance in cancer–searching for mechanisms, markers and therapeutic agents, Expert opinion on drug metabolism & toxicology, 3 (2007) 805-817.
[23] C. Viegas-Junior, A. Danuello, V. da Silva Bolzani, E.J. Barreiro, C.A.M. Fraga, Molecular hybridization: A useful tool in the design of new drug prototypes, Current medicinal chemistry, 14 (2007) 1829-1852.
[24] G. Bérubé, An overview of molecular hybrids in drug discovery, Expert opinion on drug discovery, 11 (2016) 281-305.
[25] A.A. Aly, E.M. El-Sheref, M.E. Bakheet, M.A. Mourad, A.B. Brown, S. Bräse, M. Nieger, M.A. Ibrahim, Synthesis of novel 1, 2-bis-quinolinyl-1, 4-naphthoquinones: ERK2 inhibition, cytotoxicity and molecular docking studies, Bioorganic chemistry, 81 (2018) 700-712.
[26] A.A. Aly, E.M. El-Sheref, M.E. Bakheet, M.A. Mourad, S. Bräse, M.A. Ibrahim, M. Nieger, B.K. Garvalov, K.N. Dalby, T.S. Kaoud, Design, synthesis and biological evaluation of fused naphthofuro [3, 2-c] quinoline-6, 7, 12-triones and pyrano [3, 2-c] quinoline-6, 7, 8, 13-tetraones derivatives as ERK inhibitors with efficacy in BRAF-mutant melanoma, Bioorganic chemistry, 82 (2019) 290-305.
[27] A.A. Aly, A.A. Hassan, N.K. Mohamed, L.E. Abd El-Haleem, S. Bräse, M. Polamo, M. Nieger, A.B. Brown. Synthesis of New Fused Heterocyclic 2-Quinolones and 3-Alkanonyl-4-Hydroxy-2-Quinolone. Molecules, 24 (2019) 3782-3795
[28] M. Abass, Chemistry of substituted quinolinones. Part II synthesis of novel 4-pyrazolylquinolinone derivatives, Synthetic Communications, 30 (2000) 2735-2757.

[29] M. Ismail, M. Abass, M. Hassan, Chemistry of substituted quinolinones. Part VI. Synthesis and nucleophilic reactions of 4-chloro-8-methylquinolin-2(1*H*)-one and its thione analogue, Molecules, 5 (2000) 1224-1239.
[30] M. Ismail, M. Abdel-Megid, M. Hassan, Some reactions of 2-and 4-substituted 8-methylquinolin-2 (1*H*)-ones and their thio analogues, Chemical papers-slovak academy of sciences, 58 (2004) 117-125.
[31] A.A. Aly, S.M. Samia, El-S.M. N. Abdelhafez, S.M.N. Abdelhafez, W.Y. Abdelzaher, M.A. Raslan, A.E. Ahmed, K. Thabet, A.A. M. El-Reedy, A.B. Brown, S. Bräse, New quinoline-2-one/pyrazole derivatives; design, synthesis, molecular docking, anti-apoptotic evaluation, and caspase-3 inhibition assay. Bioorganic Chemistry **(**2019) 103348 (in press). https://doi.org/10.1016/j.bioorg.2019.103348
[32] H.L. Qin, J. Leng, B.G. Youssif, M.W. Amjad, M.A.G. Raja, M.A. Hussain, Z. Hussain, S.N. Kazmi, S.N.A. Bukhari, Synthesis and mechanistic studies of curcumin analog-based oximes as potential anticancer agents, Chemical biology & drug design, 90 (2017) 443-449.
[33] F. Manetti, G.A. Locatelli, G. Maga, S. Schenone, M. Modugno, S. Forli, F. Corelli, M. Botta, A combination of docking/dynamics simulations and pharmacophoric modeling to discover new dual c-Src/Abl kinase inhibitors, Journal of medicinal chemistry, 49 (2006) 3278-3286.
[34] D.J. Burgess, Anticancer drugs: Blocking RAS effects, Nature Reviews Drug Discovery, 12 (2013) 422.
[35] A.B. Gurung, A. Bhattacharjee, Significance of Ras Signaling in Cancer and Strategies for its Control, Journal-Significance of Ras Signaling in Cancer and Strategies for its Control, 2 (2015) 147-152.
[36] A. Fernández-Medarde, E. Santos, Ras in cancer and developmental diseases, Genes & cancer, 2 (2011) 344-358.
[37] Y. Kloog, A.D. Cox, RAS inhibitors: potential for cancer therapeutics, Molecular medicine today, 6 (2000) 398-402.
[38] G. Konjević, S. Radenković, A. Vuletić, K.M.i. Martinović, V. Jurišić, T. Srdic, STAT Transcription factors in tumor development and targeted therapy of malignancies, in: Oncogene and Cancer-From Bench to Clinic, IntechOpen, 2013, pp. 456-486.
[39] M. Ashrafizadeh, Z. Ahmadi, N.G. Kotla, E.G. Afshar, S. Samarghandian, A. Mandegary, A. Pardakhty, R. Mohammadinejad, G. Sethi, Nanoparticles Targeting STATs in Cancer Therapy, Cells, 8 (2019) 1158.
[40] X. Wang, P.J. Crowe, D. Goldstein, J.L. Yang, STAT3 inhibition, a novel approach to enhancing targeted therapy in human cancers (review), International journal of oncology, 41 (2012) 1181-1191.
[41] D.R. McIlwain, T. Berger, T.W. Mak, Caspase functions in cell death and disease, Cold Spring Harb Perspect Biol, 7 (2015) a026716.
[42] E.A. Prokhorova, G.S. Kopeina, I.N. Lavrik, B. Zhivotovsky, Apoptosis regulation by subcellular relocation of caspases, Scientific Reports, 8 (2018) 12199.
[43] A. Shamas-Din, J. Kale, B. Leber, D.W. Andrews, Mechanisms of action of Bcl-2 family proteins, Cold Spring Harb Perspect Biol, 5 (2013) a008714.
[44] K.J. Campbell, S.W.G. Tait, Targeting BCL-2 regulated apoptosis in cancer, Open biology, 8 (2018) 180002.
[45] M.H. Abdelrahman, A.S. Aboraia, B.G. Youssif, B.E. Elsadek, Design, synthesis and pharmacophoric model building of new 3-alkoxymethyl/3-phenyl indole-2-carboxamides with potential antiproliferative activity, Chemical biology & drug design, 90 (2017) 64-82.

[46] C.-H. Yun, T.J. Boggon, Y. Li, M.S. Woo, H. Greulich, M. Meyerson, M.J. Eck, Structures of lung cancer-derived EGFR mutants and inhibitor complexes: Mechanism of activation and insights into differential inhibitor sensitivity, Cancer cell, 11 (2007) 217-227.
[47] Fast Rigid Exhaustive Docking (FRED) Receptor, version 2.2.5; OpenEye Scientific Software, Santa Fe, NM (USA); http://www.eyesopen.com.
[48] OMEGA, version 2.5.1.4; OpenEye Scientific Software, Santa Fe, NM (USA); http://www.eyesopen.com.
[49] VIDA, version 4.1.2; OpenEye Scientific Software, Santa Fe, NM (USA); http://www.eyesopen.com.
[50] OpenEye Scientific Software, Santa Fe, NM (USA); http://www.eyesopen.com.

Arylidenes of Quinolin-2-one scaffold as Erlotinib analogues with activities against leukemia through inhibition of EGFR TK/ STAT-3 pathways

Mohammed A. I. Elbastawesy, Mohamed Ramadan, Yaseen A.M.M. El-Shaier, Ashraf A. Aly, Gamal El-Din A Abuo-Rahma

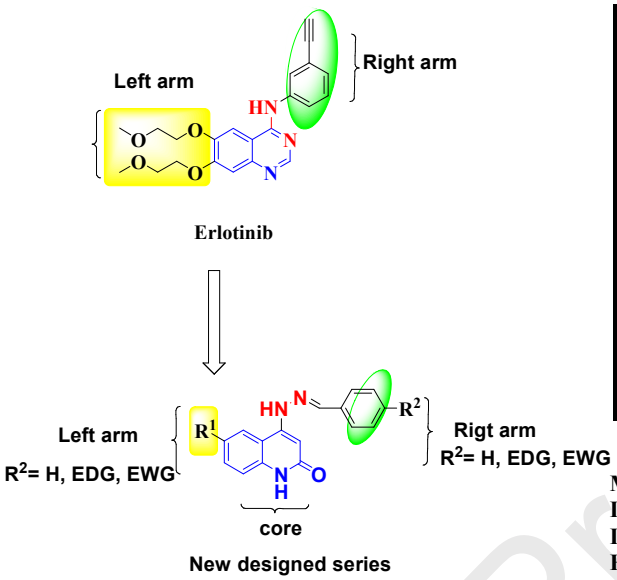

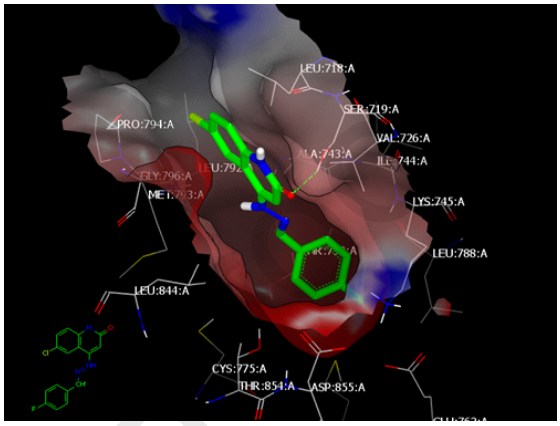

6l Docked into EGFR-TK

Medium GI_{50} = 14.94 µM (Leukemia cell line)
IC_{50} = 15.72±21 (Leukemia cells RPMI-8226)
IC_{50} = 695.49±21 nM (EGFR-TK)
H-RAS inhibition at 10.61 ng/ml using 6l/RPMI-8226.
STAT3 inhibition at 1.753±0.81 ng/ml using 6l/RPMI-8226.

Highlights

- A new series of 6-substiuted-4-(2-(4-substituted-benzylidene)hydrazinyl)quinolin-2(1*H*)-one **6a-o** have been designed and synthesized
- The structure of the synthesized compounds was proved by ^{1}H NMR, ^{13}C NMR, 2D NMR, mass and elemental analyses.
- The target compounds were evaluated for their *in vitro* cytotoxic activity against 60 cancer cell lines according to NCI protocol.
- The active compounds were further examined against the most sensitive leukemia RPMI-8226 and on healthy cell lines.
- Compound **6l** was the most active one; with IC_{50} = 15.72±1.21 and 46.05±2.36 μM against RPMI-8226 and normal cell lines, respectively.
- That compound showed a remarkable inhibitory activity compared to gefitinib
- Cell cycle analysis of RPMI-8226 cells treated with **6l** showed cell cycle arrest at G2/M phase.
- Docking studies supported the results; the study illustrated the effect of several factors on compounds activity.